MHC class II–restricted antigen presentation by plasmacytoid dendritic cells inhibits T cell–mediated autoimmunity

Magali Irla,[1] Natalia Küpfer,[1] Tobias Suter,[2] Rami Lissilaa,[3] Mahdia Benkhoucha,[1] Jonathan Skupsky,[4] Patrice H. Lalive,[1,5] Adriano Fontana,[2] Walter Reith,[1] and Stéphanie Hugues[1]

[1]Department of Pathology, University of Geneva Medical School, 1211 Geneva, Switzerland
[2]Section of Clinical Immunology, University Hospital, 8044 Zürich, Switzerland
[3]NovImmune SA, 1228 Plan-Les-Ouates, Geneva, Switzerland
[4]Center for Vascular and Inflammatory Diseases, University of Maryland School of Medicine, Baltimore, MD 21201
[5]Division of Neurology and Laboratory Medicine Service, University Hospital of Geneva, 1211 Geneva, Switzerland

Although plasmacytoid dendritic cells (pDCs) express major histocompatibility complex class II (MHCII) molecules, and can capture, process, and present antigens (Ags), direct demonstrations that they function as professional Ag-presenting cells (APCs) in vivo during ongoing immune responses remain lacking. We demonstrate that mice exhibiting a selective abrogation of MHCII expression by pDCs develop exacerbated experimental autoimmune encephalomyelitis (EAE) as a consequence of enhanced priming of encephalitogenic CD4$^+$ T cell responses in secondary lymphoid tissues. After EAE induction, pDCs are recruited to lymph nodes and establish MHCII-dependent myelin-Ag–specific contacts with CD4$^+$ T cells. These interactions promote the selective expansion of myelin-Ag–specific natural regulatory T cells that dampen the autoimmune T cell response. pDCs thus function as APCs during the course of EAE and confer a natural protection against autoimmune disease development that is mediated directly by their ability to present of Ags to CD4$^+$ T cells in vivo.

CORRESPONDENCE
W. Reith:
Walter.reith@unige.ch
OR
S. Hugues:
Stephanie.hugues@unige.ch

Abbreviations used: Ag, antigen; cDC, conventional DC; CNS, central nervous system; dLN, draining LN; EAE, experimental autoimmune encephalomyelitis; MOG, myelin oligodendrocyte glycoprotein; MS, multiple sclerosis; pDCs, plasmacytoid DCs; SC, spinal cord; TEC, thymic epithelial cell.

Conventional DCs (cDCs) play well established roles in the induction of immunity and tolerance. Both functions require antigen (Ag)-specific interactions between T cells and cDCs in secondary lymphoid tissues. The outcome of these interactions depends on the modulation and integration of three signals: TCR engagement by peptide–MHC complexes, the recruitment of costimulatory and adhesion molecules, and the delivery of soluble mediators (Lebedeva et al., 2005). Under steady-state conditions, cDCs reside in peripheral tissues and lymphoid organs in an immature state characterized by low cell surface expression of MHC class II (MHCII), costimulatory, and adhesion molecules. Immature cDCs continuously capture and present self-Ags, circulate from tissues to lymphoid organs, and maintain tolerance by inducing the deletion of autoreactive T cells or the development of regulatory T cells (T reg cells; Steinman et al., 2003). Signals associated with inflammation, infections, or tissue damage induce cDC maturation, a process involving complex phenotypical changes, including the up-regulation of MHCII, costimulatory, and adhesion molecules, the secretion of inflammatory mediators, and altered migratory properties. Activation of naive T cells by mature cDCs results in clonal expansion and differentiation into effector and memory T cells.

Plasmacytoid DCs (pDCs) constitute a unique DC subtype found mainly in the blood and secondary lymphoid organs. The activation of pDCs by infections triggers the secretion of large quantities of type I IFN, suggesting that they have crucial innate functions (Colonna et al., 2004). However, pDCs also express MHCII molecules and undergo a maturation process similar to that of cDCs (Villadangos and Young, 2008). Furthermore, pDCs can internalize, process, and

W. Reith and S. Hugues contributed equally to this paper.

The Rockefeller University Press $30.00
J. Exp. Med. Vol. 207 No. 9 1891-1905
www.jem.org/cgi/doi/10.1084/jem.20092627

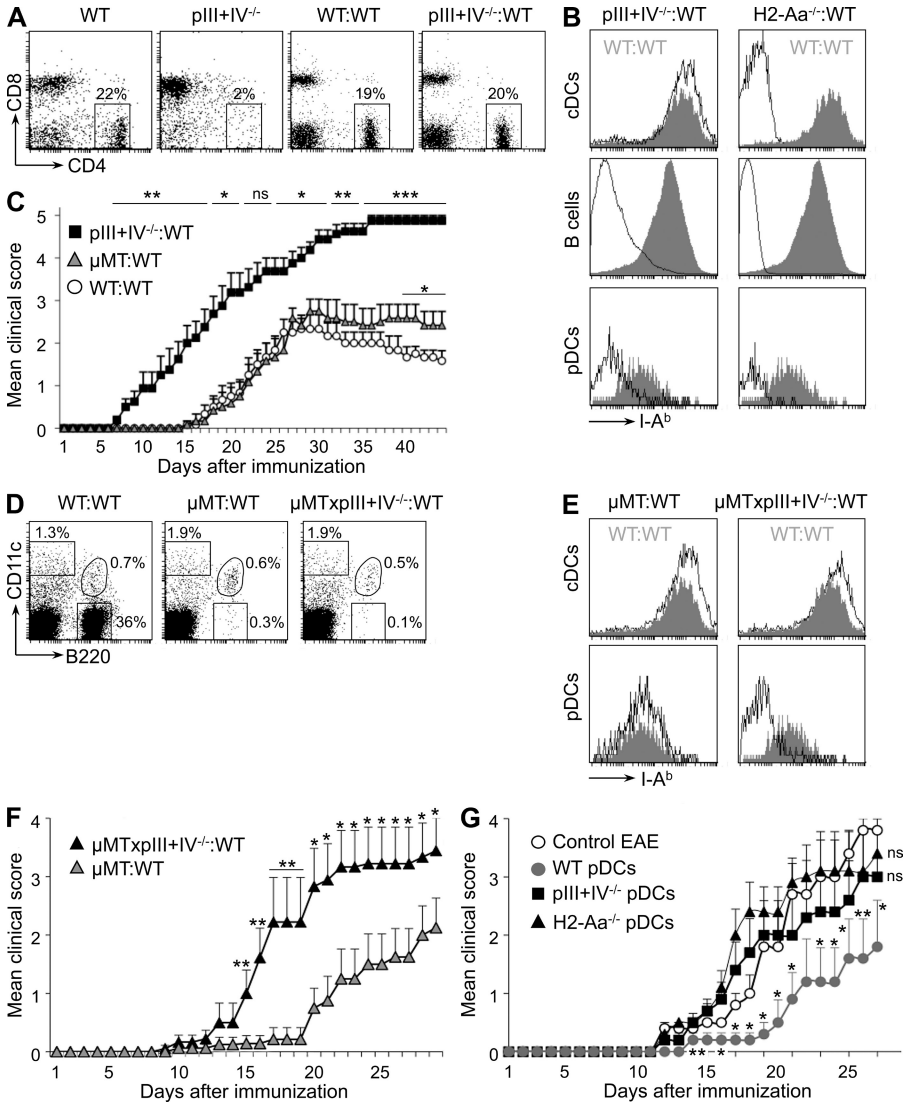

Figure 1. EAE is exacerbated in mice lacking MHCII expression by pDCs. (A) LN cells from WT:WT and pIII+IV$^{-/-}$:WT chimeras and control WT and pIII+IV$^{-/-}$ mice were analyzed by flow cytometry for the presence of CD4$^+$ T cells. Percentages of CD4$^+$ T cells are indicated. Results are representative of 10 experiments, each with at least three mice per group. (B) MHCII (I-A^b) expression by LN cDCs, B cells, and pDCs was analyzed by flow cytometry for pIII+IV$^{-/-}$:WT, H2-Aa$^{-/-}$:WT, and WT:WT chimeras. Results are representative of five experiments, each with at least three mice per group. (C) EAE was induced by immunization with MOG$_{35-55}$+CFA in pIII+IV$^{-/-}$:WT ($n = 8$), μMT:WT ($n = 6$), and WT:WT ($n = 6$) chimeras. Results are representative of three experiments. The means and SEM are shown. ns, not significant; *, $P < 0.05$; **, $P < 0.01$; ***, $P < 0.001$. (D) LN cells from WT:WT, μMT:WT, and μMTxpIII+IV$^{-/-}$:WT chimeras were analyzed by flow cytometry for the expression of CD11c and B220. The percentages of B220$^+$ B cells, CD11c^{hi} cDCs, and CD11c^{int}B220$^+$ pDCs are indicated. Results are representative of three experiments, each with at least three mice per group. (E) MHCII (I-A^b) expression by LN cDCs and pDCs was analyzed by flow cytometry for μMT:WT, μMTxpIII+IV$^{-/-}$:WT, and WT:WT chimeras. Results are representative of three experiments, each with at least three mice per group. (F) EAE was induced by immunization with MOG$_{35-55}$+CFA in μMTxpIII+IV$^{-/-}$:WT and μMT:WT chimeras. Results are representative of two experiments. The means and SEM derived from six mice per group are shown. **, $P < 0.01$; *, $P < 0.05$. (G) pDCs from WT, pIII+IV$^{-/-}$, and H2-Aa$^{-/-}$ mice were incubated with MOG$_{35-55}$ and transferred into WT recipients. EAE was induced 1 d after the transfer by immunization with MOG$_{35-55}$. Results are representative of two independent experiments. The means and SEM derived from five mice per group are shown. **, $P < 0.01$; *, $P < 0.05$.

present Ags to CD4$^+$ T cells and cross-present Ags to CD8$^+$ T cells (Hoeffel et al., 2007; Sapoznikov et al., 2007; Di Pucchio et al., 2008; Young et al., 2008). These findings had suggested that pDCs can function as APCs. However, whether pDCs indeed function as APCs in vivo during ongoing immune responses, and whether this promotes T cell–mediated immunity and/or the maintenance of self-tolerance, remained unsolved issues.

pDCs can participate in the maintenance of peripheral tolerance. The induction of T reg cells by pDCs was shown to confer tolerance to cardiac allografts, prevent asthmatic reactions to inhaled Ags, and protect against graft versus host disease (de Heer et al., 2004; Ochando et al., 2006; Hadeiba et al., 2008). pDCs can also induce tolerance by promoting deletion of pathogenic T cells (Goubier et al., 2008) or inhibiting effector CD4$^+$ T cell responses in a relapsing model of experimental autoimmune encephalomyelitis (EAE; Bailey-Bucktrout et al., 2008). As these studies relied mainly on antibody-mediated ablation of pDCs, they could not discriminate between innate and adaptive functions of these cells. It therefore remained unknown if pDCs function as tolerogenic APCs in these systems.

We have investigated whether MHCII-mediated Ag presentation by pDCs instructs CD4$^+$ T cell responses during EAE, a mouse model for multiple sclerosis (MS; Wekerle, 2008). EAE induced by immunization with myelin oligodendrocyte glycoprotein (MOG) was found to be severely exacerbated in mice exhibiting a selective abrogation of MHCII expression by pDCs. Conversely, EAE was dampened by the adoptive transfer of WT, but not MHCII-deficient, pDCs. EAE induction triggered the recruitment of pDCs to LNs, where they engaged in MHCII-dependent and MOG-specific interactions with CD4$^+$ T cells. This inhibited the development of pathogenic T cells during the priming phase of the disease

Table I. Increased incidence of clinical EAE at early time points in mice lacking MHCII expression by pDCs and B cells

Chimeras	Day 12	Day 16	Day 20	Day 24
WT:WT	0/6 (0%)	2/6 (33%)	4/6 (67%)	6/6 (100%)
pIII+IV$^{-/-}$:WT	5/8 (62%), ***	8/8 (100%), ***	8/8 (100%), **	8/8 (100%), NA
μMT:WT	0/6 (0%), NA	1/6 (17%), ns	4/6 (67%), ns	5/6 (83%), ns

EAE was induced by immunization with MOG_{35-55}+CFA in WT:WT, pIII+IV$^{-/-}$:WT, and μMT:WT chimeras. The numbers and percentages of mice that developed disease at days 12, 16, 20, and 24 are provided. P-values for disease incidence were calculated relative to WT:WT mice using the χ^2 test. ns, not significant; **, P < 0.01; ***, P < 0.001; NA, not applicable.

by promoting the selective expansion of natural T reg cells. Our results demonstrate that Ag-presentation by pDCs can inhibit T cell–mediated autoimmunity and can thus determine the outcome of adaptive immune responses in vivo.

RESULTS

Generation of mice lacking MHCII expression by pDCs and B cells

The gene encoding the MHCII transactivator (CIITA), which regulates all qualitative and quantitative aspects of MHCII expression, is controlled by three cell type–specific promoters called pI, pIII, and pIV (Reith et al., 2005) (Fig. S1 A). pI drives CIITA expression in macrophages, microglial cells, and all cDC subsets. pIII drives CIITA expression in pDCs and B cells. pIV is essential for CIITA expression in thymic epithelial cells (TECs) and cells of nonhematopoietic origin stimulated with IFN-γ. The differential dependence of cDCs and pDCs on pI and pIII allowed us to use mice lacking pIII and pIV (pIII+IV$^{-/-}$; LeibundGut-Landmann et al., 2004) to study the role of MHCII-restricted Ag presentation by pDCs.

MHCII expression was analyzed by flow cytometry on cDCs (CD11c^{hi}B220^{-}), pDCs (CD11c^{int}B220^{+}PDCA-1^{+}), and B cells (CD11c^{-}B220^{+}) isolated from LNs of WT, pIII+IV$^{-/-}$, and MHCII-deficient (H2-Aa$^{-/-}$) mice (Fig. S1, B and C). MHCII expression by pDCs and B cells was abrogated in pIII+IV$^{-/-}$ mice to levels similar to those observed in H2-Aa$^{-/-}$ mice. Conversely, cDCs retained WT levels of MHCII expression in pIII+IV$^{-/-}$ mice.

Similar levels of IFN-α4 mRNA expression and IFN-α4 secretion were induced in vivo in WT and pIII+IV$^{-/-}$ mice in response to viral infection (Fig. S2 A). Furthermore, ex vivo LN pDCs from WT, pIII+IV$^{-/-}$, and H2-Aa$^{-/-}$ mice produced equivalent amounts of IFN-α4 in response to in vitro stimulation with CpG-A (Fig. S2 B). The latter result was confirmed using BM-derived pDCs (BM-pDCs; Fig. S2 C). In addition, activated BM-pDCs from WT, pIII+IV$^{-/-}$, and H2-Aa$^{-/-}$ mice produced similar amounts of IL-6 and TNF (Fig. S2 C) and failed to secrete detectable levels of IL-12, IL-10, and MCP-1 (not depicted). These results indicated that neither the deficiency in CIITA nor the absence of MHCII expression led to intrinsic defects in the production of type I IFN or other cytokines by pDCs.

pIV drives CIITA expression in cortical TECs and is hence required for positive selection of CD4^{+} T cells (Waldburger et al., 2003; Irla et al., 2008). pIII+IV$^{-/-}$ mice therefore lack CD4^{+} T cells. To circumvent this defect, we generated BM chimeras in which irradiated WT mice were reconstituted with BM from pIII+IV$^{-/-}$ mice. Normal percentages of CD4^{+} T cells were restored in the LNs and blood of pIII+IV$^{-/-}$:WT chimeras compared with WT:WT control chimeras (Fig. 1 A and not depicted). MHCII expression by pDCs and B cells remained as negative in pIII+IV$^{-/-}$:WT chimeras as in H2-Aa$^{-/-}$:WT controls (Fig. 1 B and not depicted). In contrast, cDCs exhibited WT levels of MHCII expression in pIII+IV$^{-/-}$:WT chimeras (Fig. 1 B). pIII+IV$^{-/-}$:WT chimeras thus differ from WT:WT controls exclusively with respect to MHCII expression by pDCs and B cells.

Exacerbation of EAE in mice lacking MHCII expression by pDCs

EAE was induced in pIII+IV$^{-/-}$:WT and WT:WT chimeras by immunization with MOG_{35-55} peptide in the presence of CFA. EAE induction did not restore MHCII expression by pDCs and B cells in pIII+IV$^{-/-}$:WT chimeras (Fig. S3 A). Disease onset was significantly accelerated and clinical symptoms were markedly aggravated in pIII+IV$^{-/-}$:WT chimeras relative to WT:WT controls. (Fig. 1 C and Table I).

2 d after EAE induction, pDCs in pIII+IV$^{-/-}$:WT and WT:WT chimeras expressed similarly levels of IFN-α4 mRNA (Fig. S3 B). After 14 d, pDCs in pIII+IV$^{-/-}$:WT chimeras exhibited a twofold increase in IFN-α4 mRNA relative to pDCs in WT:WT chimeras (Fig. S3 B). However, this modest increase was probably an indirect consequence of the strongly enhanced inflammation and exacerbated disease observed at this time point (Fig. 1 C; Table I; and see Fig. 3, C–F) because neither CIITA-deficient nor MHCII-deficient pDCs exhibited intrinsic alterations with respect to IFN-α4 production (Fig. S2). Moreover, EAE development in WT mice was not significantly affected by the injection of a dose of IFN-α (5 ng) that corresponds to the serum concentration detected in mice with EAE (Isaksson et al., 2009) or a 10-fold greater dose (50 ng) that boosts the serum concentration to the high levels induced by viral infections (Fig. S3 C). These results suggested that EAE exacerbation in pIII+IV$^{-/-}$:WT chimeras cannot be accounted for by the slight increase in IFN-α production by pDCs.

To investigate the respective contributions of Ag presentation of pDCs and B cells, we performed EAE experiments with μMT:WT chimeras, which lack B cells (Hjelmström et al., 1998; Fig. 1 D) but exhibit normal MHCII expression by pDCs (Fig. 1 E). In marked contrast to pIII+IV$^{-/-}$:WT chimeras, EAE was not accelerated or aggravated at peak disease in μMT:WT chimeras (Fig. 1 C and Table I). In accordance with previous studies (Fillatreau et al., 2002; Lampropoulou et al., 2008;

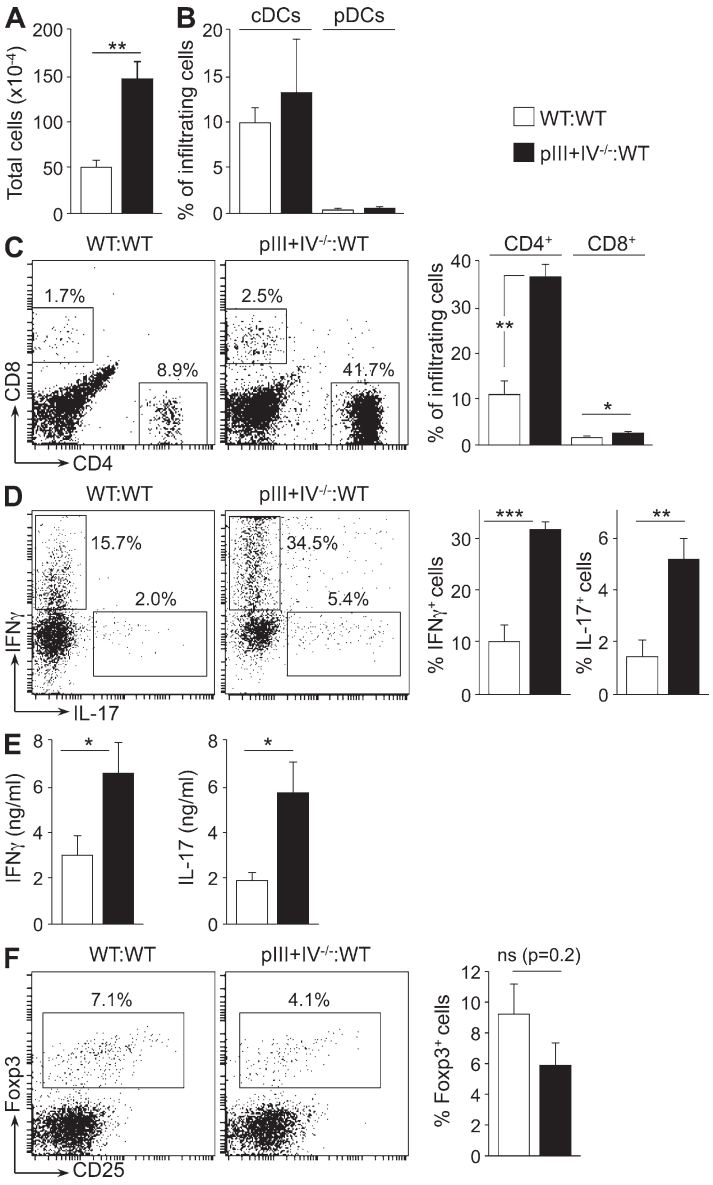

Figure 2. SC infiltration by pathogenic $MOG_{35–55}$–specific $CD4^+$ T cells is increased in mice lacking MHCII expression by pDCs. EAE was induced in WT:WT and pIII+$IV^{-/-}$:WT chimeras, and cells infiltrating the SCs were harvested after 25 d. (A) Absolute numbers of total SC-infiltrating cells. (B) The percentages of SC-infiltrating cells corresponding to cDCs and pDCs were quantified by flow cytometry. (C) Representative flow cytometry profiles and histograms representing the percentages of SC-infiltrating $CD4^+$ and $CD8^+$ T cells are shown. (D) SC-infiltrating cells were restimulated in vitro with $MOG_{35–55}$, and $CD4^+$ T cells expressing IFN-γ and IL-17 were quantified by flow cytometry. Representative flow cytometry profiles and histograms representing the percentages of $CD4^+$ T cells expressing IFN-γ and IL-17 are shown. (E) Secretion of IFN-γ and IL-17 into the culture supernatant was quantified for $MOG_{35–55}$-restimulated SC-infiltrating cells. (F) $CD4^+$ T cells expressing CD25 and Foxp3 were quantified by flow cytometry in SC-infiltrating cells. Representative flow cytometry profiles and a histogram representing the percentages of $CD4^+$ T cells expressing Foxp3 are shown. Bar graphs show the means and SEM derived from two independent experiments, each with at least three mice per group. ns, not significant; *, $P < 0.05$; **, $P < 0.01$; ***, $P < 0.001$.

Matsushita et al., 2008), μMT:WT chimeras did exhibit a significant aggravation of the disease during the recovery phase (Fig. 1 C). However, this effect was minor compared with the dramatically altered disease course observed in pIII+$IV^{-/-}$:WT chimeras, suggesting that the latter was a consequence of deficient MHCII expression by pDC rather than B cells. These results nevertheless needed to be interpreted with caution because MHCII-deficient B cells remained present in pIII+$IV^{-/-}$:WT chimeras, whereas B cells were absent in μMT:WT chimeras. We therefore generated μMTxpIII+$IV^{-/-}$ mice and compared EAE development between μMTxpIII+$IV^{-/-}$:WT and μMT:WT chimeras, which both lack B cells (Fig. 1 D) and differ only with respect to MHCII expression by pDCs (Fig. 1 E). EAE was markedly accelerated and aggravated in μMTxpIII+$IV^{-/-}$:WT chimeras compared with μMT:WT chimeras (Fig. 1 F), confirming that deficient MHCII expression by pDCs is responsible for disease exacerbation.

We next performed pDC transfer experiments to demonstrate that MHCII expression by pDCs confers protection against EAE. $MOG_{35–55}$-loaded BM-pDCs from WT, pIII+$IV^{-/-}$, or H2-$Aa^{-/-}$ mice were transfered into WT mice 1 d before EAE induction. EAE was significantly dampened in mice that had received WT pDCs (Fig. 1 G). In contrast, no improvement was observed in mice that had received pIII+$IV^{-/-}$ or H2-$Aa^{-/-}$ pDCs (Fig. 1 G). pDC-mediated protection against EAE is thus dependent on their expression of MHCII molecules.

To confirm that pDCs indeed function as APCs during EAE, we induced the disease with MOG protein rather than $MOG_{35–55}$ peptide. EAE induced with MOG protein was significantly exacerbated in pIII+$IV^{-/-}$:WT chimeras compared with WT:WT controls (Fig. S3 D), indicating that MHCII-sufficient pDCs can attenuate disease severity by capturing, processing, and presenting myelin Ags in vivo.

Enhanced infiltration of the central nervous system (CNS) by MOG-specific $CD4^+$ T cells in mice lacking MHCII expression by pDCs

Histological examinations of the spinal cord (SC) performed 25 d after induction of EAE revealed that disease exacerbation in pIII+$IV^{-/-}$:WT chimeras correlated with increased numbers of demyelinated areas (Fig. S4 A), inflammatory foci (Fig. S4 B), and infiltrating $CD3^+$ T cells (Fig. S4 C). Flow cytometry experiments confirmed that absolute numbers of infiltrating cells were markedly increased in pIII+$IV^{-/-}$:WT chimeras (Fig. 2 A). The percentages of infiltrating cells corresponding to cDCs and pDCs were very similar between pIII+$IV^{-/-}$:WT and WT:WT chimeras (Fig. 2 B). Infiltrating $CD8^+$ T cells were scarce, and their frequency was increased only modestly in pIII+$IV^{-/-}$:WT chimeras (Fig. 2 C). In contrast, the percentage of infiltrating $CD4^+$ T cells was

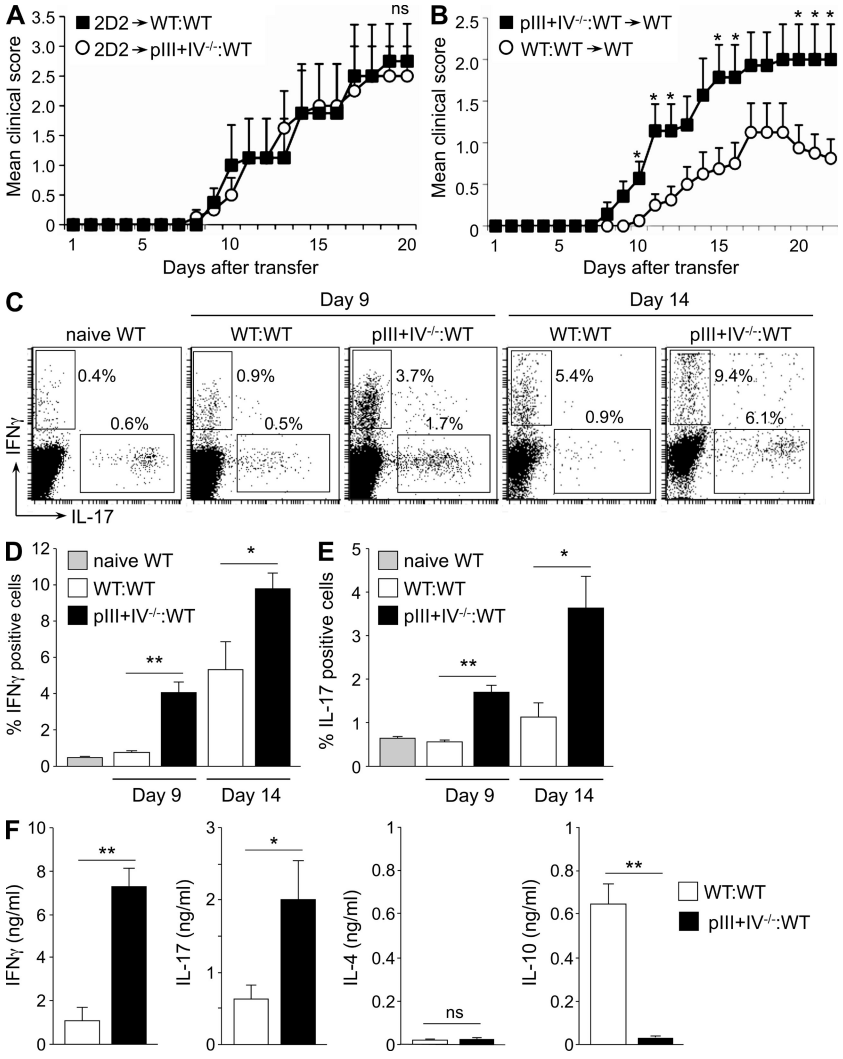

Figure 3. Priming of pathogenic $MOG_{35–55}$-specific CD4+ T cells is increased in LNs of mice lacking MHCII expression by pDCs. (A) Effector $MOG_{35–55}$-specific CD4+ T cells were generated from 2D2 mice and adoptively transferred into WT:WT and pIII+$IV^{-/-}$:WT chimeras. Results are representative of two experiments. The means and SEM derived from four mice per group are shown. (B) Effector $MOG_{35–55}$-specific CD4+ T cells were generated from $MOG_{35–55}$-immunized WT:WT or pIII+$IV^{-/-}$:WT chimeras and adoptively transferred into WT mice. Results show the mean and SEM derived from two experiments with a total of seven or eight mice per group. *, $P < 0.05$. (C–E) EAE was induced by immunization with $MOG_{35–55}$+CFA in WT:WT and pIII+$IV^{-/-}$:WT chimeras. dLN cells isolated 9 and 14 d after immunization were restimulated in vitro with $MOG_{35–55}$ and analyzed by flow cytometry for the expression of CD4, IFN-γ, and IL-17. (C) Representative flow cytometry profiles analyzing IFN-γ and IL-17 expression by CD4+ T cells are shown. Percentages of CD4+ T cells expressing IFN-γ and IL-17 are indicated. (D and E) Histograms represent the percentages of CD4+ T cells expressing IFN-γ (D) or IL-17 (E). Results show the mean and SEM derived from two independent experiments with at least three mice per group. *, $P < 0.05$; **, $P < 0.01$. (F) Concentrations of IFN-γ, IL-17, IL-4, and IL-10 were measured in culture supernatants from $MOG_{35–55}$-restimulated LN cells isolated 14 d after induction of EAE. Results show the means and SEM derived from two independent experiments, each with at least three mice per group. ns, not significant; *, $P < 0.05$; **, $P < 0.01$.

markedly increased in pIII+$IV^{-/-}$:WT chimeras (Fig. 2 C). In vitro restimulation assays using exogenous $MOG_{35–55}$-loaded APCs indicated that the SC-infiltrating CD4+ T cells contained increased numbers of $MOG_{35–55}$-specific effector cells expressing IFN-γ or IL-17 (Fig. 2 D). The concentrations of these cytokines were consequently increased in the culture supernatants of $MOG_{35–55}$-restimulated T cells isolated from the SCs of pIII+$IV^{-/-}$:WT chimeras (Fig. 2 E). Similar results were obtained when the restimulation assays were repeated with total SC cells containing endogenous APCs (unpublished data).

Enhanced cellular inflammation (Fig. S5 A) and increased numbers of CD4+ T cells (Fig. S5 B) were also observed in the SCs of μMTxpIII+$IV^{-/-}$:WT chimeras compared with μMT:WT controls. CD4+ T cells isolated from the SCs of μMTxpIII+$IV^{-/-}$:WT chimeras secreted more IFN-γ and IL-17 in response to in vitro restimulation with $MOG_{35–55}$ (Fig. S5, C and D).

The fraction of SC-infiltrating CD4+ T cells corresponding to Foxp3+ T reg cells tended to be reduced in pIII+$IV^{-/-}$:WT chimeras compared with WT:WT controls (Fig. 2 F). Similarly, the percentage of SC-infiltrating CD4+ T cells corresponding to T reg cells was reduced in μMTxpIII+$IV^{-/-}$:WT chimeras relative to μMT:WT controls (Fig. S5 E).

Enhanced infiltration of the SC by pathogenic CD4+ T cells could not be attributed to altered MHCII expression by microglial cells, which up-regulated MHCII expression equally during EAE in pIII+$IV^{-/-}$:WT and WT:WT chimeras (Fig. S6). This is consistent with the fact that CIITA expression in microglia relies on promoter pI of the CIITA gene (Suter et al., 2000; Reith et al., 2005).

Collectively, these results indicated that EAE exacerbation in mice lacking MHCII expression by pDCs correlates mainly with strongly increased infiltration of the CNS by $MOG_{35–55}$-specific Th1 and Th17 cells. The latter is consistent with the fact that Th1 and Th17 cells are believed to be the major pathogenic cells in EAE (Steinman et al., 2002; Murphy et al., 2003; Langrish et al., 2005).

Enhanced priming of encephalitogenic CD4+ T cells in mice lacking MHCII expression by pDCs

Adoptive transfer EAE experiments were performed to discriminate between potential roles of MHCII expression by pDCs during the effector phase in the CNS and the priming phase in secondary lymphoid tissues. To study the contribution

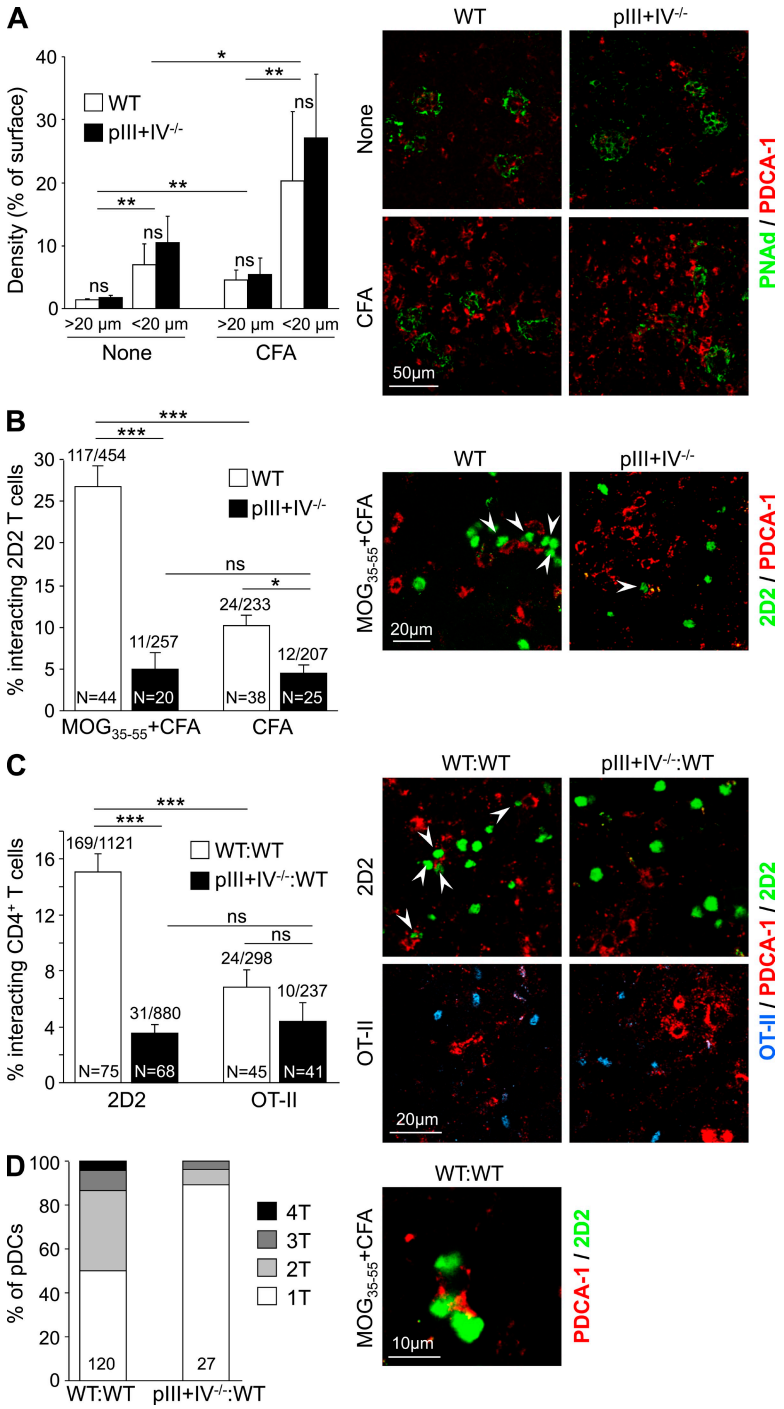

Figure 4. pDCs recruited to LNs during EAE establish Ag-specific interactions with CD4+ T cells. (A) WT and pIII+IV$^{-/-}$ mice were injected with CFA and dLNs were harvested after 2 d. dLN sections from untreated and CFA-treated mice were stained with antibodies against PNAd to label HEVs and PDCA-1 to label pDCs. Histograms show the density (percentage of surface) of pDCs in regions situated near to (<20 µm) or distant from (>20 µm) HEVs. Results are representative of three independent experiments. The means and SEM derived from three independent mice per group are shown. ns, not significant; *, $P < 0.05$; **, $P < 0.01$. 7–12 confocal images were analyzed for each genotype and region. Representative images are shown. (B) CMTMR-labeled 2D2 CD4+ T cells were adoptively transferred into WT and pIII+IV$^{-/-}$ mice that had been injected 1 d previously with $MOG_{35–55}$+CFA or CFA alone. dLNs were harvested 1 d after the T cell transfer, and sections were stained with antibodies against PDCA-1. Histograms show the percentages of 2D2 T cells that interact with pDCs and show the mean and SEM derived from at least two independent experiments. ns, not significant; *, $P < 0.05$; ***, $P < 0.001$. The numbers of confocal images analyzed (N) are indicated at the bottom of each bar. The ratios above the bars represent the number of interacting 2D2 T cells over the total number of 2D2 T cells. Representative images are shown for $MOG_{35–55}$+CFA-treated WT and pIII+IV$^{-/-}$ mice. Arrowheads indicate 2D2 T cells that interact with pDCs. (C and D) CMTMR-labeled 2D2 or OT-II T cells were adoptively transferred into WT:WT and pIII+IV$^{-/-}$:WT chimeras that had been immunized 1 d previously with $MOG_{35–55}$+CFA. dLNs were harvested 1 d after the T cell transfer, and sections were stained with antibodies against PDCA-1. (C) The histogram shows the percentages of 2D2 or OT-II T cell that interact with pDCs and shows the mean and SEM derived from at least two independent experiments. ***, $P < 0.001$; ns, not significant. The numbers of confocal images analyzed (N) are indicated at the bottom of each bar. The ratios above the bars represent the number of interacting CD4+ T cells over the total number of CD4+ T cells. Representative images from WT:WT and pIII+IV$^{-/-}$:WT chimeras are shown. Arrowheads indicate 2D2 T cells interacting with pDCs. (D) The histogram shows the distribution of pDCs in contact with one, two, three, or four 2D2 T cells. The numbers of pDCs that were analyzed are indicated above the bars. A representative image of a pDC interacting with three different 2D2 T cells in the LN of a WT:WT chimera is shown.

of MHCII expression by pDCs during the effector phase, $MOG_{35–55}$-specific CD4+ T cells isolated from 2D2 TCR transgenic mice were activated in vitro with $MOG_{35–55}$-loaded APCs and transferred into pIII+IV$^{-/-}$:WT and WT:WT chimeras. The incidence, time course, and severity of EAE were indistinguishable between the pIII+IV$^{-/-}$:WT and WT:WT recipients (Fig. 3 A). To study the contribution of MHCII expression by pDCs to encephalitogenic T cell priming, equal numbers of CD4+ T cells purified from the LNs of $MOG_{35–55}$-immunized pIII+IV$^{-/-}$:WT and WT:WT chimeras were transferred into WT recipients. Mice that had received CD4+ T cells from the pIII+IV$^{-/-}$:WT chimeras developed EAE with an earlier onset and increased severity (Fig. 3 B). These results suggested that MHCII expression by pDCs confers protection against EAE by inhibiting the priming of encephalitogenic T cells in secondary lymphoid tissues but has no evident impact on the subsequent effector phase in the CNS.

In vitro T cell restimulation assays were next used to measure the frequencies of $MOG_{35–55}$-specific IFN-γ– and IL-17–secreting CD4+ T cells in the LNs of WT:WT and pIII+IV$^{-/-}$:WT chimeras at days 9 and 14 after EAE induction. At both time points, IFN-γ– and IL-17–secreting $MOG_{35–55}$-specific CD4+ T cells were significantly more

frequent in pIII+IV$^{-/-}$:WT chimeras (Fig. 3, C–E). The concentrations of IFN-γ and IL-17 were also greater in the culture supernatants of restimulated T cells from the pIII+IV$^{-/-}$:WT chimeras (Fig. 3 F). In contrast, IL-4 production was low and not significantly affected. Enhanced $MOG_{35–55}$-specific Th1 and Th17 development in pIII+IV$^{-/-}$:WT chimeras was therefore not associated with an impaired Th2 response. Interestingly, a decrease in the immunosuppressive cytokine IL-10 was detected in the culture supernatants of T cells isolated from pIII+IV$^{-/-}$:WT chimeras (Fig. 3 F). These results suggested that MHCII expression by pDCs attenuates the priming of encephalitogenic Th1 and Th17 CD4$^+$ T cells, possibly through a mechanism implicating IL-10–dependent inhibition.

pDCs recruited to LNs during EAE engage in Ag-specific contacts with CD4$^+$ T cells

Staining of sections with antibodies against PDCA-1 indicated that immunization with CFA induced the recruitment of pDCs to the T cell zone of the draining LNs (dLNs) within 2 d (Fig. 4 A). pDCs were preferentially localized near HEVs in both immunized and nonimmunized mice. No significant differences in pDC recruitment or localization were observed between WT and pIII+IV$^{-/-}$ mice (Fig. 4 A). To assess the ability of these pDCs to establish Ag-specific contacts with CD4$^+$ T cells, $MOG_{35–55}$-specific CD4$^+$ T cells purified from 2D2 mice were labeled with CMTMR and transferred into WT or pIII+IV$^{-/-}$ mice that had been immunized 1 d previously with $MOG_{35–55}$+CFA or CFA alone. Contacts between the 2D2 T cells and PDCA-1$^+$ pDCs were quantified in dLN sections 24 h after the transfer. 26.9 ± 2.4% of the 2D2 T cells were found in close proximity to pDCs in the dLNs of $MOG_{35–55}$+CFA–immunized WT mice, whereas this fraction was only 4.9 ± 1.3% in the dLNs of $MOG_{35–55}$+CFA–immunized pIII+IV$^{-/-}$ mice (Fig. 4 B). Furthermore, only 10.2 ± 1.9% of the 2D2 T cells interacted with pDCs in the dLNs of WT mice injected with CFA alone. These results indicated that pDCs recruited to the dLNs during EAE establish frequent contacts with 2D2 T cells in a $MOG_{35–55}$–specific and MHCII-dependent manner. In mice injected with CFA alone, significantly more 2D2 T cells were found close to pDCs in WT mice (10.2 ± 1.9%) than in pIII+IV$^{-/-}$ mice (4.4 ± 1.2%), suggesting that the 2D2 T cells scan pDCs for the presence of their cognate MHCII–Ag complexes (Fig. 4 B).

The establishment of Ag-specific and MHCII-dependent contacts between pDCs and 2D2 T cells in the dLNs during EAE was next documented using pIII+IV$^{-/-}$:WT and WT:WT chimeras. CMTMR-labeled 2D2 T cells or control OT-II T cells were transferred into the chimeras after the induction of EAE by immunization with $MOG_{35–55}$. A strong recruitment of pDCs to the dLNs was again observed 48 h after immunization (unpublished data). The frequency of $MOG_{35–55}$-specific 2D2 T cells that interacted with pDCs was fivefold higher in WT:WT chimeras (15.1 ± 1.3%) than in pIII+IV$^{-/-}$:WT chimeras (3.5 ± 0.6%; Fig. 4 C). The frequency of 2D2 T cells interacting with WT:WT pDCs was significantly higher than the frequency observed for the irrelevant OT-II T cells (Fig. 4 C). Finally, the proportion of pDCs that interact with multiple 2D2 T cells was higher in WT:WT chimeras than in pIII+IV$^{-/-}$:WT chimeras (Fig. 4 D). pDCs interacting with multiple OT-II T cells were not observed in either WT:WT or pIII+IV$^{-/-}$:WT chimeras (unpublished data). Collectively, these results suggested that induction of EAE leads to recruitment of pDCs to the dLNs, where they localize preferentially around HEVs and establish Ag-specific and MHCII-dependent interactions with $MOG_{35–55}$-specific CD4$^+$ T cells.

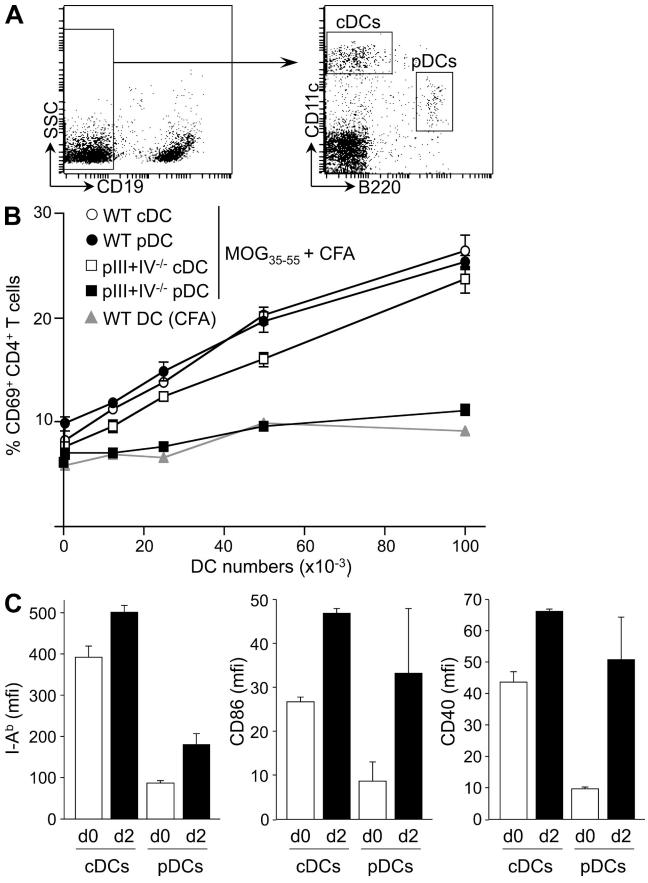

Figure 5. pDCs present $MOG_{35–55}$ during EAE. (A and B) LN cells were pooled from 8–10 WT and pIII+IV$^{-/-}$ mice that had been immunized 2 d previously with $MOG_{35–55}$+CFA or CFA alone. The cells were then stained with antibodies against CD19, CD11c, and B220, and cDCs (CD19$^-$CD11c^{hi}B220$^-$ cells) and pDCs (CD19$^-$CD11c^{int}B220$^+$ cells) were purified by sorting. (A) Representative flow cytometry profiles are shown to illustrate the labeling and purification of pDCs and cDCs. (B) Variable numbers of purified cDCs and pDCs were incubated for 18 h with 2D2 T cells. The percentages of activated CD69^{hi} CD4$^+$ 2D2 T cells were then quantified by flow cytometry. Results are representative of two experiments. The graph shows the means and SEM derived from two experiments. (C) MHCII (I-A^b), CD86, and CD40 expression was analyzed by flow cytometry on cDCs and pDCs isolated from the dLNs of WT mice that had been immunized 2 d previously with $MOG_{35–55}$+CFA. cDCs and pDCs isolated from the LNs of nonimmunized WT mice (day 0) were used as controls. The histograms represent the mean fluorescence intensity (mfi) and SEM derived from two experiments.

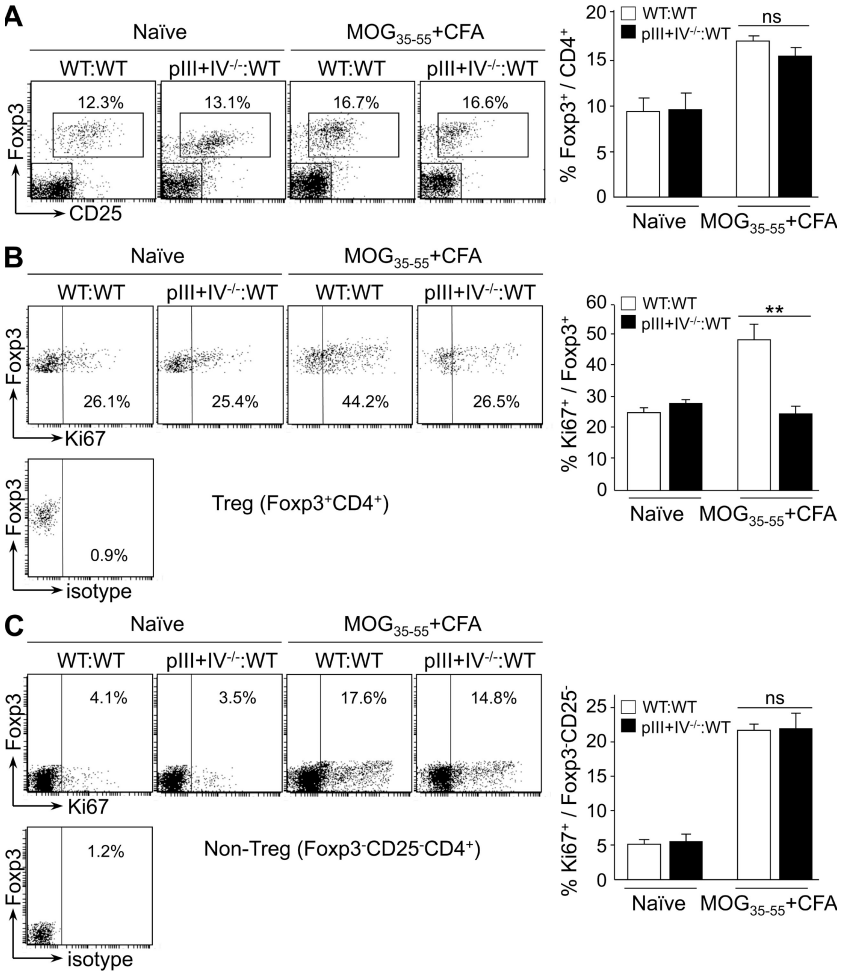

Figure 6. Defective T reg cell proliferation in mice lacking MHCII expression pDCs. (A–C) WT:WT and pIII+IV$^{-/-}$:WT chimeras were immunized with MOG_{35-55}+CFA. Nonimmunized (naive) chimeras were used as controls. dLNs were harvested 14 d later and analyzed by flow cytometry. (A) CD25 and Foxp3 expression by CD4+ T cells was analyzed. Representative flow cytometry profiles are shown, with percentages of Foxp3+ T reg cells indicated. The histogram shows the means and SEM derived from three experiments, each with three mice per group. ns, not significant. (B) Frequencies of proliferating Ki67+ cells were determined in the Foxp3+ CD4+ T reg cell population. Representative flow cytometry profiles are shown, with percentages of Ki67+ T reg cells indicated. The Ki67+ gate was defined relative to staining with an isotype control. The histogram shows the means and SEM derived from three experiments, each with three mice per group. **, $P < 0.01$. (C) Frequencies of proliferating Ki67+ cells were determined in the CD25$^-$Foxp3$^-$ (non–T reg cell) CD4+ T cell population. Representative flow cytometry profiles are shown, with percentages of Ki67+ cells indicated. The Ki67+ gate was defined relative to staining with an isotype control. The histogram shows the means and SEM derived from three experiments, each with three mice per group. ns, not significant. (D) IL-10 and TGF-β1 mRNA levels were quantified by quantitative RT-PCR in CD4+ T cells purified from the dLNs of WT:WT and pIII+IV$^{-/-}$:WT chimeras 14 d after immunization with MOG_{35-55}+CFA. CD4+ T cells purified from LNs of nonimmunized (naive) WT:WT chimeras were used as a reference. The means and SEM were derived from three to four measurements, each made with three mice per group. *, $P < 0.05$.

pDCs function as APCs during EAE

To confirm that pDCs present MOG_{35-55} during EAE, they were purified from the dLNs of WT and pIII+IV$^{-/-}$ mice 48 h after immunization with MOG_{35-55}+CFA (Fig. 5 A). cDCs were purified in parrallel. Variable numbers of pDCs and cDCs were incubated with MOG_{35-55}–specific 2D2 T cells and T cell activation was measured by examining the expression of CD69 (Fig. 5 B). cDCs from WT and pIII+IV$^{-/-}$ mice activated 2D2 T cells with equal efficiency. pDCs from WT mice activated 2D2 T cells as efficiently as cDCs. In contrast, pDCs from pIII+IV$^{-/-}$ mice were unable to induce 2D2 T cell activation above the background level observed for DCs isolated from mice immunized with CFA alone. In agreement with their ability to function as efficient APCs, dLN pDCs isolated from WT mice 2 d after EAE induction up-regulated MHCII, CD86, and CD40 expression in a manner similar to that of cDCs (Fig. 5 C). pDCs can thus indeed function as competent APCs that present MOG_{35-55} in vivo during EAE.

Impaired T reg cell expansion during EAE in mice lacking MHCII expression by pDCs

The finding that MHCII-mediated Ag presentation by pDCs inhibits encephalitogenic CD4+ T cell responses during EAE suggested that pDCs might promote the development of CD4+ T reg cells. T reg cell populations were therefore analyzed in naive and MOG_{35-55}–immunized pIII+IV$^{-/-}$:WT and WT:WT chimeras. The frequency of Foxp3+ T reg cells in total LN CD4+ T cells was identical between naive pIII+IV$^{-/-}$:WT and WT:WT chimeras (Fig. 6 A). This was also true for Foxp3+ T reg cells in blood (Fig. S7A). 14 d after the induction of EAE, the percentage of T reg cells increased to an equal extent in pIII+IV$^{-/-}$:WT and WT:WT chimeras (Fig. 6 A). The absence of MHCII expression by pDCs, therefore, did not have a major impact on total T reg cell frequencies.

Proliferation in the Foxp3+ CD4+ T reg cell population was quantified by analyzing the expression of Ki67 (Gerdes et al., 1984). No difference in the frequency of proliferating

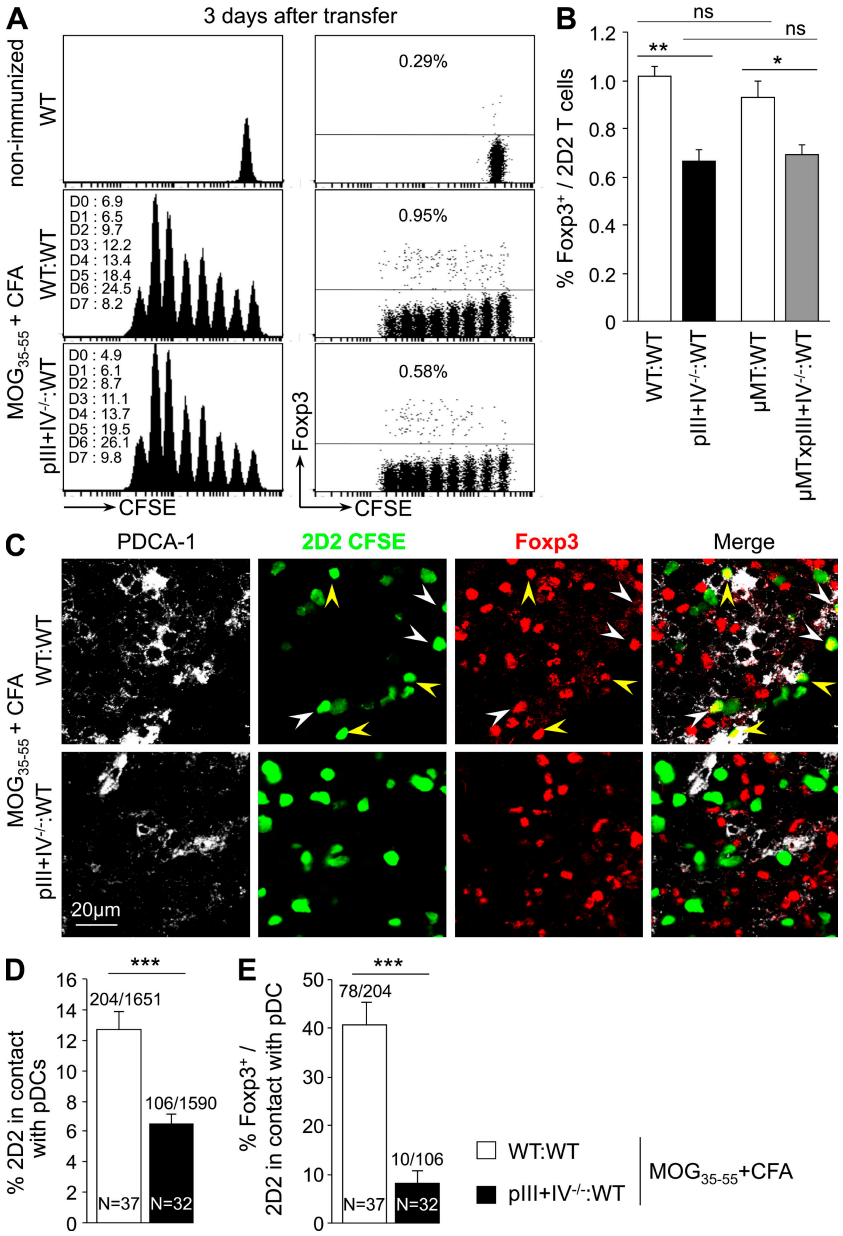

Figure 7. Ag presentation by pDCs induces T reg cell development. (A) CD4+ T cells were purified from the LNs of 2D2 mice, labeled with CFSE, and transferred into WT:WT and pIII+IV$^{-/-}$:WT chimeras that had been immunized 1 d previously with $MOG_{35–55}$+CFA. Nonimmunized WT recipients were used as controls. 3 d after transfer, 2D2 T cells in the LNs were analyzed by flow cytometry for dilution of CFSE labeling (left and right) and the frequency of Foxp3+ cells (right). Percentages of cells in the peaks corresponding to divisions 0–7 (D0–D7) are indicated on the left. Percentages of Foxp3+ cells are indicated on the top and right. The results are representative of two independent experiments. (B) CD4+ T cells were purified from the LNs of 2D2 mice, labeled with CFSE, and transferred into WT:WT, pIII+IV$^{-/-}$:WT, μMT:WT, and μMTxpIII+IV$^{-/-}$:WT chimeras that had been immunized 1 d previously with $MOG_{35–55}$+CFA. 3 d after transfer, 2D2 T cells in the dLNs were analyzed by flow cytometry to determine the frequency of Foxp3+ T reg cells. The results are representative of two independent experiments. The means and SEM were derived from three chimeras per group. ns, not significant; *, $P < 0.05$; **, $P < 0.01$. (C) CD4+ T cells were purified from LNs of 2D2 mice, labeled with CFSE, and transferred into WT:WT and pIII+IV$^{-/-}$:WT chimeras that had been immunized 1 d previously with $MOG_{35–55}$+CFA. 3 d after transfer, dLN sections were stained using antibodies against PDCA-1 and Foxp3. Representative images derived from two independent experiments are shown. Arrowheads indicate CFSE+ Foxp3+ 2D2 T reg cells; circles indicate CFSE+ Foxp3+ 2D2 T reg cells that interact with pDCs. (D) The histogram shows the percentages of CFSE+ 2D2 T cells that interact with pDCs. The ratios above the bars represent the number of interacting 2D2 T cells over the total number of 2D2 T cells. (E) The histograms show the percentages of Foxp3+ T reg cells among CFSE+ 2D2 T cells found in close proximity to pDCs. The ratios above the bars represent the number of Foxp3+ 2D2 T cells over the number of 2D2 T cells interacting with pDCs. (D and E) The number of confocal images analyzed (N) is indicated at the bottom of each bar. Results were pooled from two independent experiments with two mice per group. Histograms show the means and SEM derived from two independent experiments with two mice per group. ***, $P < 0.001$.

T reg cells was observed in LNs between naive pIII+IV$^{-/-}$:WT and WT:WT chimeras (Fig. 6 B). As described previously (Darrasse-Jèze et al., 2009), this homeostatic T reg cell proliferation was markedly greater than that of non–T reg CD4+ T cells (Fig. 6 C). After immunization with $MOG_{35–55}$, the percentage of proliferating T reg cells in LNs increased significantly in WT:WT chimeras but remained unchanged in pIII+IV$^{-/-}$:WT chimeras (Fig. 6 B). The frequency of proliferating T reg cells in immunized pIII+IV$^{-/-}$:WT mice was not significantly greater than the basal level observed in naive mice (Fig. 6 B). The defect in immunization-induced proliferation was restricted to T reg cells because no difference in proliferation of non–T reg CD4+ T cells was observed between pIII+IV$^{-/-}$:WT and WT:WT chimeras (Fig. 6 C).

Immunization-induced T reg cell proliferation was also impaired in the spleen of pIII+IV$^{-/-}$:WT chimeras (Fig. S7 B). In contrast, it was not observed in the SCs of pIII+IV$^{-/-}$:WT chimeras (Fig. S7 C), suggesting that T reg cell restimulation in the CNS is mediated by APCs other than pDCs, such as cDCs, macrophages or microglia, which retain MHCII expression in pIII+IV$^{-/-}$:WT chimeras. This experiment also confirmed that MHCII-mediated Ag presentation by pDCs does not control T cell responses in the CNS.

Proliferating T reg cells are more efficient at suppressing T cell responses than resting T reg cells (Klein et al., 2003). In agreement with this, IL-10 and TGF-β1 mRNA levels in CD4+ T cells purified from LNs after EAE induction were

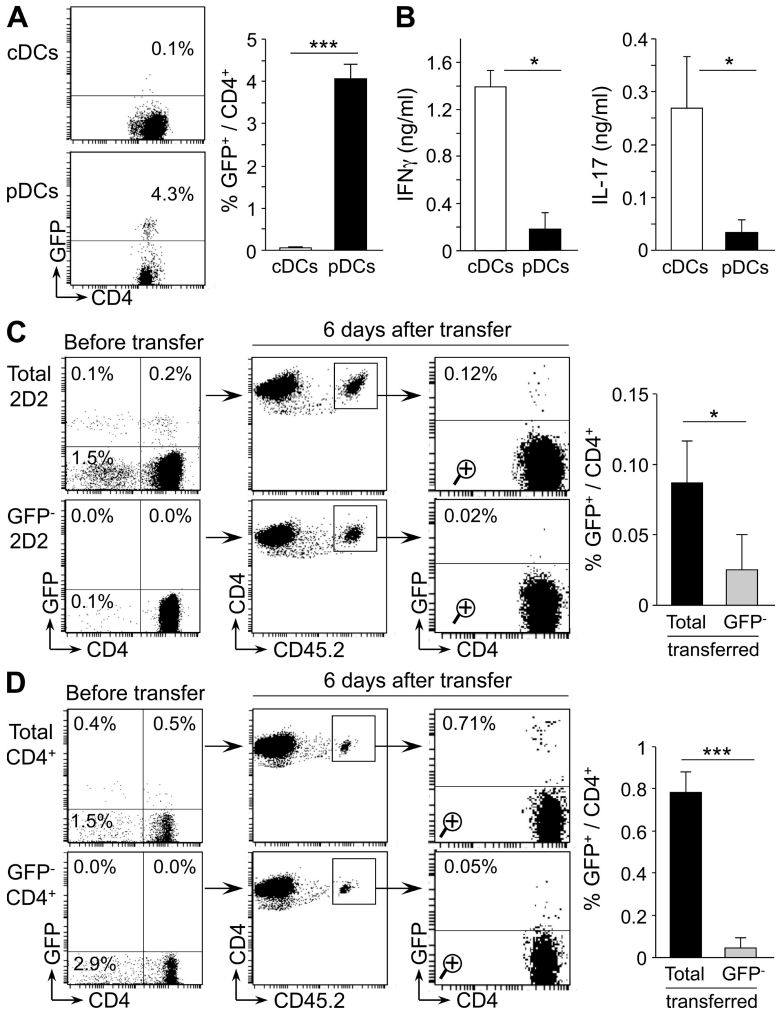

Figure 8. pDCs promote the selective expansion of natural T reg cells. (A and B) BM pDCs ($CD11c^{int}B220^{+}PDCA\text{-}1^{+}$) or BM cDCs ($CD11c^{hi}B220^{-}PDCA\text{-}1^{-}$) were isolated from WT mice, loaded with MOG_{35-55} and activated with CpG-A plus CpG-B or LPS, respectively. The DCs were then used to stimulate $CD4^{+}$ T cells isolated from 2D2 × Foxp3-GFP mice. (A) The frequencies of GFP^{+} T reg cells were analyzed in the $CD4^{+}$ T cell population after 96 h of stimulation. Representative flow cytometry profiles are shown, with percentages of GFP^{+} T reg cells indicated. The histogram shows the percentages of GFP^{+} T reg cells in the $CD4^{+}$ 2D2 T cell population. The means and SEM were derived from three experiments. ***, $P < 0.001$. (B) Concentrations of IFN-γ and IL-17 were measured in the culture supernatants. The histogram shows the means and SEM derived from three experiments. *, $P < 0.05$. (C) Total or GFP^{-} $CD4^{+}$ T cells were purified from 2D2 × Foxp3-GFP $CD45.2^{+}$ donors (left profiles) and transferred into CD45.1 hosts. The recipient mice were immunized 1 d after the transfer with MOG_{35-55}+CFA. dLN cells isolated 6 d after the transfer were analyzed by flow cytometry for the frequency of $CD45.2^{+}$ 2D2 cells in the total $CD4^{+}$ T cell population (middle profiles) and for GFP expression in $CD4^{+}CD45.2^{+}$ 2D2 T cells (right profiles). Zoomed views are shown in the right profiles to facilitate visualization of the minor GFP^{+} T reg cell populations. The results are representative of two experiments. The means and SEM were derived from three mice per group. *, $P < 0.05$. (D) Total or GFP^{-} $CD4^{+}$ T cells were purified from Foxp3-GFP $CD45.2^{+}$ donors (left profiles) and transferred into CD45.1 hosts. The recipient mice were immunized 1 d after the transfer with MOG_{35-55}+CFA. dLN cells isolated 6 d after the transfer were analyzed by flow cytometry for the frequency of $CD45.2^{+}$ donor cells in the total $CD4^{+}$ T cell population (middle profiles) and for GFP expression in the donor $CD4^{+}CD45.2^{+}$ T cells (right profiles). Zoomed views are shown in the right profiles to facilitate visualization of the minor GFP^{+} T reg cell populations. The results are representative of two experiments. The means and SEM were derived from three mice per group. ***, $P < 0.001$.

significantly lower in $pIII{+}IV^{-/-}$:WT chimeras than in WT:WT controls (Fig. 6 D).

Impaired Ag-specific T reg cell expansion in mice lacking MHCII expression by pDCs

Adoptive transfer experiments were performed with $CD4^{+}$ T cells purified from 2D2 mice to determine whether impaired immunization-induced T reg cell expansion in $pIII{+}IV^{-/-}$:WT chimeras would affect MOG_{35-55}-specific T reg cells. $CD4^{+}$ 2D2 T cells were labeled with CFSE and transferred into MOG_{35-55}-immunized $pIII{+}IV^{-/-}$:WT and WT:WT chimeras. Naive WT mice were used as control recipients. $CFSE^{+}$ 2D2 T cells present in LNs were analyzed 3 d after transfer for their proliferation and expression of Foxp3. Although 2D2 T cells did not proliferate in nonimmunized mice, they proliferated massively and to a similar extent in immunized $pIII{+}IV^{-/-}$:WT and WT:WT chimeras (Fig. 7 A). The frequency of $Foxp3^{+}$ T reg cells within the proliferating 2D2 T cell population was significantly reduced in $pIII{+}IV^{-/-}$:WT chimeras relative to WT:WT controls (Fig. 7, A and B).

To exclude a role of B cells, the 2D2 T cell transfer experiments were repeated with μMTxpIII+$IV^{-/-}$:WT and μMT:WT chimeras. The frequency of $Foxp3^{+}$ T reg cells in the proliferating 2D2 T cell population was again reduced in μMTxpIII+$IV^{-/-}$:WT chimeras relative to μMT:WT controls (Fig. 7 B), confirming that impaired expansion of 2D2 T reg cells resulted from the loss of MHCII expression by pDCs. B cells appeared to have little or no impact on 2D2 T reg cell expansion because the frequencies of 2D2 T reg cells were similar between WT:WT and μMT:WT chimeras and between $pIII{+}IV^{-/-}$:WT and μMTxpIII+$IV^{-/-}$:WT chimeras.

Staining of LN sections at day 3 confirmed that 2D2 T cells interacted less frequently with pDCs in $pIII{+}IV^{-/-}$:WT chimeras than in WT:WT controls (Fig. 7, C and D). $Foxp3^{+}$ cells were also markedly less enriched among 2D2 T cells located in close proximity to pDCs in $pIII{+}IV^{-/-}$:WT chimeras than in WT:WT controls (Fig. 7, C and E). Finally, the frequencies of $Foxp3^{+}$ 2D2 T cells were globally greater in our analysis of LN sections (Fig. 7, D and E) than when they were quantified by flow cytometry (Fig. 7, A and B). This is consistent with the fact that our analysis of LN sections

focused on pDC-rich areas and therefore selected for regions enriched in T reg cells retained by contacts with pDCs.

To assess the ability of pDCs to promote $MOG_{35–55}$-specific T reg cell expansion we performed in vitro restimulation assays with 2D2 T cells purified from 2D2 × Foxp3-GFP mice and mature $MOG_{35–55}$-loaded pDCs. $MOG_{35–55}$-loaded cDCs were used as control APCs. The frequency of GFP^+ T reg cells induced in the 2D2 T cell population was markedly greater when pDCs were used as the APCs (Fig. 8 A). Conversely, the development of Th1 and Th17 cells, as assessed by the secretion of IFN-γ and IL-17 into the supernatant, was markedly greater with cDCs (Fig. 8 B). Collectively, these results support the model that MHCII-mediated presentation of $MOG_{35–55}$ by pDCs favors the expansion of $MOG_{35–55}$-specific T reg cells.

Induction of EAE promotes the expansion of natural T reg cells

T reg cell expansion during EAE could be the result of proliferation of natural T reg cells or differentiation of T reg cells from non–T reg cell precursors. To distinguish between these two possibilities, total or GFP^- $CD4^+$ T cells were purified from 2D2 × Foxp3-GFP $CD45.2^+$ mice and transferred into WT $CD45.1^+$ hosts. The recipient mice were then immunized with $MOG_{35–55}$ and 2D2 T cell populations were analyzed in the dLNs after 6 d. Both total and GFP^- 2D2 T cells expanded extensively in the immunized mice (Fig. 8 C). The frequencies of GFP^+ 2D2 T reg cells in the immunized mice were significantly greater in recipients that had received total 2D2 T cells than in those that had received GFP^- 2D2 T cells (Fig. 8 C). This suggested that 2D2 T reg cell development resulted from the expansion of preexisting T reg cells rather than from de novo differentiation of T reg cells from non–T reg cells. However, 2D2 T reg cell frequencies in the immunized mice were very low, probably as a result of massive proliferation of non–T reg 2D2 cells. We therefore repeated the transfer experiments with total and GFP^- polyclonal $CD4^+$ T cells from Foxp3-GFP mice. As reported previously using this approach (Korn et al., 2007), GFP^+ T reg cell frequencies were significantly higher in recipients that had received total $CD4^+$ T cells than in those that had received GFP^- $CD4^+$ T cells (Fig. 8 D). This confirmed that T reg cell expansion in response to induction of EAE is due mainly to the expansion of preexisting natural T reg cells.

MHCII expression by pDCs is required for the expansion of T reg cells capable of inhibiting EAE

T reg cell transfer experiments were performed to determine whether disease exacerbation in pIII+$IV^{-/-}$:WT chimeras is a direct consequence of impaired T reg cell expansion. $CD4^+$ $CD25^+$ T reg cells were isolated from the dLNs of $MOG_{35–55}$-immunized WT:WT or pIII+$IV^{-/-}$:WT chimeras. These cells, which are predominantly $Foxp3^+$ (Fig. 9 A), were transferred into WT hosts. EAE was then induced in the recipient mice. The transfer of T reg cells derived from immunized WT:WT chimeras strongly attenuated EAE severity in the recipients (Fig. 9 B and Table S1). In contrast, the transfer of T reg cells derived from immunized pIII+$IV^{-/-}$:WT chimeras did not alter the disease course (Fig. 9 B and Table S1). MHCII expression by pDCs is thus required for the generation of suppressive T reg cells capable of attenuating EAE.

DISCUSSION

Although pDCs can capture, process, and present Ags, whether they actually function as APCs capable of shaping the outcome of T cell responses in vivo by presenting Ags to naive T cells during ongoing adaptive immune responses remained unknown. Studies relying on antibody-mediated depletion of pDCs had indicated that pDCs can stimulate T cell priming (Isaksson et al., 2009) or promote the induction of T cell tolerance (de Heer et al., 2004; Bailey-Bucktrout et al., 2008; Jongbloed et al., 2009). However, because these studies were based on pDC ablation they could not discriminate between the contributions of innate and adaptive functions of pDCs. Activated pDCs are known to be major sources of type I IFNs and other inflammatory cytokines. These soluble mediators can have profound impacts on the outcome of T cell activation. It was therefore crucial to determine to what extent Ag presentation by pDCs influences the outcome of immune responses in vivo.

Our study provides several lines of evidence demonstrating that pDCs function as APCs that regulate the priming phase of EAE. First, early after disease onset, LN $CD4^+$ T cells from chimeras lacking MHCII expression by pDCs were

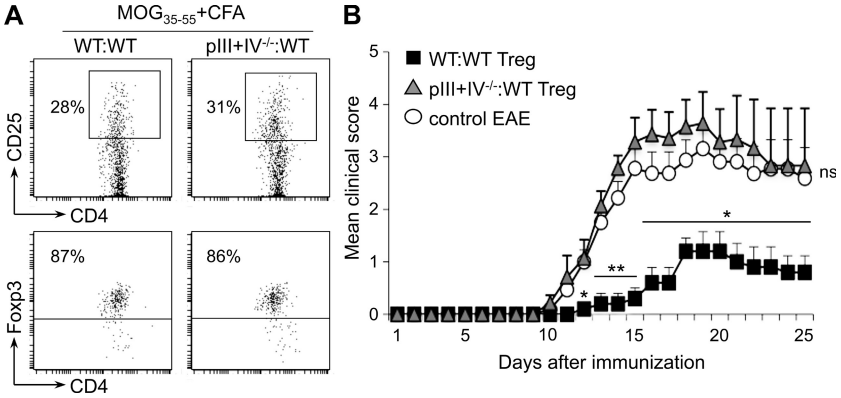

Figure 9. pDCs promote the expansion of T reg cells capable of attenuating EAE. $CD4^+CD25^+$ T reg cells were purified from the LNs of $MOG_{35–55}$+CFA-immunized WT:WT or pIII+$IV^{-/-}$:WT chimeras and transferred into WT recipients. 1 d after the transfer, EAE was induced in the recipients by immunization with $MOG_{35–55}$+CFA. (A) Representative flow cytometry profiles are shown to illustrate the expression of CD4, CD25, and Foxp3 by the purified T reg cells. Percentages of $CD25^+$ and $Foxp3^+$ cells are indicated. (B) Results from two experiments were pooled. The means and SEM were derived from at least six mice per group. ns, not significant; *, $P < 0.05$; **, $P < 0.01$.

markedly enriched in pathogenic $MOG_{35–55}$-specific IFN-γ– and IL-17–secreting T cells, and these cells exhibited a significantly increased capacity to transfer the disease to WT recipients. Second, the induction of EAE promoted a rapid recruitment of pDCs to LNs, where they concentrated in the vicinity of HEVs. Thus, as demonstrated for cDCs (Bajénoff et al., 2003), pDCs recruited to the LNs are strategically positioned for being scanned efficiently by incoming T cells. Third, EAE induction promoted the establishment of MHCII-dependent and Ag-specific interactions between $CD4^+$ T cells and pDCs in LNs. Fourth, LN pDCs purified from $MOG_{35–55}$–immunized mice were as efficient as cDCs in activating $MOG_{35–55}$–specific $CD4^+$ T cells ex vivo in the absence of added exogenous $MOG_{35–55}$ peptide. Fifth, pDCs purified from the LNs after induction of EAE exhibited an activated phenotype characterized by increased cell surface expression of MHCII and T cell costimulatory molecules. The latter is consistent with the fact that pDCs can activate T cells efficiently provided they undergo maturation (Villadangos and Young, 2008). Finally, EAE was exacerbated in chimeras lacking MHCII expression by pDCs after active immunization not only with $MOG_{35–55}$ peptide but also with MOG protein, suggesting that MHCII-sufficient pDCs can capture, process, and present myelin Ags in vivo. Collectively, these results indicate that pDCs can function as true APCs in vivo.

Antibody-mediated depletion of pDCs was recently reported to lead to disease aggravation in EAE (Bailey-Bucktrout et al., 2008). Because pDCs were ablated in this system, it was not possible to determine whether disease exacerbation was a result of the abrogation of Ag presentation by pDCs or if it was a result of altered production of soluble mediators such as type I IFNs. We found that WT and MHCII-deficient pDCs exhibit similar intrinsic abilities to produce type I IFNs and other cytokines. Furthermore, EAE was dampened by the adoptive transfer of WT pDCs but not by MHCII-deficient pDCs. Lastly, the administration of IFN-α did not alter the course of EAE. Collectively, these results demonstrate that pDCs attenuate EAE by presenting Ags to $CD4^+$ T cells rather than via their innate functions.

In naive mice, total T reg cell numbers and frequencies of proliferating T reg cells were indistinguishable between WT mice and mice lacking MHCII expression by pDCs. As described previously (Darrasse-Jèze et al., 2009), this suggests that homeostatic proliferation of T reg cells under steady-state conditions is dependent on cell types other than pDCs, such as cDCs. In contrast to naive mice, a clear increase in T reg cell proliferation was evident upon EAE induction in the spleens and LNs of WT mice compared with mice lacking MHCII expression by pDCs. In agreement with a previous study demonstrating that actively dividing T reg cells are more suppressive than quiescent T reg cells (Klein et al., 2003), impaired T reg cell proliferation in chimeras lacking MHCII expression by pDCs was associated with decreased production of suppressive cytokines. As documented by an earlier study (Korn et al., 2007), T reg cell proliferation during EAE was found to reflect the expansion of preexisting natural $Foxp3^+$ T reg cells rather than the expansion of T reg cells newly derived from $Foxp3^-CD4^+$ T cells. Finally, disease exacerbation in mice lacking MHCII expression by pDCs was a direct consequence of the impaired induction of a T reg cell population capable of suppressing EAE. These results demonstrated that MHCII-mediated Ag presentation by pDCs protects against the development of EAE by promoting a selective expansion of Ag-specific $Foxp3^+$ T reg cells.

The difference in T reg cell proliferation observed between WT and mutant chimeras did not lead to a difference in the frequency of total LN T reg cells. This probably reflects the exit of T reg cells from the secondary lymphoid tissues and their migration to the CNS. MOG-specific $Foxp3^+$ T reg cells traffic readily to the CNS (Korn et al., 2007). This previous study also found that T reg cell numbers did not change significantly in peripheral lymphoid compartments during EAE. Migration of the newly expanded T reg cells to the CNS is also consistent with the finding that the reduction in proliferating LN T reg cell numbers in mutant chimeras correlates with a decrease in the frequency of T reg cells infiltrating the SC.

The frequency of T reg cells infiltrating the SC of mice lacking MHCII expression by pDCs was reduced only modestly. Furthermore, in contrast to T reg cells found in the spleen and LNs, the frequency of proliferating T reg cells was not reduced in the SCs of the mutant chimeras. These observations could be explained by the fact that T reg cell proliferation in the CNS can be sustained by Ag restimulation by microglial cells (Aloisi, 2001) or infiltrating cDCs and macrophages, which retain normal MHCII expression in our mutant chimeras. This would be consistent with previous studies showing that these APCs can restimulate encephalitogenic $CD4^+$ T cells in the CNS (Wekerle et al., 1987; Greter et al., 2005; Bailey et al., 2007).

A change in the number and function of MOG-specific T reg cells in the CNS has been reported to coincide with EAE recovery (Korn et al., 2007). This suggested that TCR engagement of myelin-specific T reg cells is required for their relocation to the CNS and their reactivation in situ. In agreement with this, we also observed an increase in T reg cells in the SC of WT mice during the recovery phase that follows peak disease (unpublished data). However, the recruitment and activity of T reg cells is unlikely to be under the control of Ag presentation by pDCs localized in the CNS because our adoptive-transfer experiments indicated that the effector phase of EAE is not altered in mice lacking MHCII expression by pDCs.

Collectively, our results support the model that MHCII-mediated presentation of myelin Ags by pDCs in secondary lymphoid tissues confers natural protection against EAE because it favors the selective expansion of natural T reg cells capable of suppressing the priming and/or expansion of pathogenic IL-17– and IFN-γ–secreting effector $CD4^+$ T cells. It may be relevant that contact duration of in vitro interactions between $CD4^+$ T cells and pDCs was found to be considerably shorter than for interactions between $CD4^+$

T cells and cDCs (unpublished data). Because the dynamics of T cell interactions with APCs are known to contribute to the functional outcome T cell stimulation (Hugues et al., 2006), an intriguing possibility is that brief contacts with pDCs favor T reg cell development.

MS patients exhibit impaired peripheral T reg cell functions (O'Connor and Anderton, 2008). In addition, pDCs exhibiting impaired maturation have been described in MS patients (Pashenkov et al., 2001; Stasiolek et al., 2006; Lande et al., 2008). This suggests that the mechanism we have uncovered in the context of EAE may also be relevant for the human disease, raising the hope that our findings may pave the way for the development of novel therapeutic strategies. For instance, the transfer of myelin-Ag–loaded pDCs or approaches designed to expand and activate pDCs would favor the presentation of CNS-derived Ags by pDCs, thus stimulating T reg cell induction by pDCs, and eventually might benefit MS patients.

MATERIALS AND METHODS

Mice. All mice had a pure C57BL/6 background and were maintained under SPF conditions. C57BL/6 (CD45.1 or CD45.2) mice were maintained in our animal facility. pIII+IV$^{-/-}$ (LeibundGut-Landmann et al., 2004), μMT (Kitamura et al., 1991), H2-Aa$^{-/-}$ (Köntgen et al., 1993), OT-II (Barnden et al., 1998), 2D2 (Bettelli et al., 2003), and Foxp3-GFP (Skupsky et al., 2010) mice have been previously described. All animal husbandry and experiments were approved by and performed in accordance with guidelines from the animal research committee of the University of Geneva.

BM chimeras. BM from tibia and femurs was recovered by flushing with PBS-EDTA, dissociated by repeated passages through a 20-gauge needle, and red cells were lysed. 7×10^6 cells were injected intravenously into irradiated (900 rad) recipients. Reconstitution was assessed by analyzing blood cells by flow cytometry after 6–8 wk.

EAE experiments. EAE was induced by active immunization with 100 μg $MOG_{35–55}$ (MEVGWYRSPFSRVVHLYRNGK; Biotrend) or 200 μg of recombinant mouse MOG (aa 1–121; Urich et al., 2006). Recombinant mouse MOG was provided by B. Becher (University Hospital of Zurich, Zurich, Switzerland). Mice received subcutaneous injections in both flanks of $MOG_{35–55}$ or recombinant MOG emulsified in incomplete Freund adjuvant (Sigma-Aldrich) supplemented with 500 μg/ml *Mycobacterium tuberculosis* (BD). Mice were also injected with 100 ng pertussis toxin (Sigma-Aldrich) into the tail vein at days 0 and 2. EAE symptoms were scored as follows: 1, flaccid tail; 2, impaired righting reflex and hind limb weakness; 3, partial hind limb paralysis; 4, complete hind limb paralysis; 5, hind limb paralysis with partial fore limb paralysis; 6, moribund. Intravenous injections with 5 or 50 ng IFN-α (Miltenyi Biotec) were done on the same day as induction of EAE. Adoptive transfer EAE experiments with encephalitogenic CD4$^+$ T cells from chimeric mice were performed as follows. Mice were immunized with $MOG_{35–55}$+CFA on day 0, rechallenged with $MOG_{35–55}$+CFA on day 7, and dLNs and spleens were harvested on day 11. CD4$^+$ T cells were purified and incubated for 3 d with 10 μg/ml $MOG_{35–55}$ and irradiated T cell–depleted splenocytes from naive mice. Live cells were isolated using Lympholyte M gradient (Cedarlane Laboratories) and 5×10^6 cells were injected into the tail vein of recipient mice.

Adoptive transfer EAE experiments with encephalitogenic CD4$^+$ T cells from 2D2 mice were performed as follows. LN cells from 2D2 mice were incubated for 5 d with 10 μg/ml $MOG_{35–55}$ in the presence of 2.5 ng/ml of recombinant mouse IL-18 (MBL). CD4$^+$ T cells were purified, live cells were isolated using Lympholyte M gradient, and 5×10^6 cells were injected into the tail vein of recipient mice. EAE symptoms in adoptive transferred EAE were scored as for EAE induced by immunization.

Adoptive transfer of T reg cells was performed as follows. Chimeric mice were immunized with $MOG_{35–55}$+CFA, dLNs were harvested after 10 d, and 2×10^5 purified CD4$^+$CD25$^+$ T cells were injected into the tail vein of recipient WT mice. EAE was then induced by immunization of the recipients with $MOG_{35–55}$+CFA.

Adoptive transfer of pDCs was performed as follows. 6×10^5 BM-pDCs loaded with $MOG_{35–55}$ were transferred into WT recipients. EAE was then induced by immunization with $MOG_{35–55}$+CFA.

Secretion of IFN-α induced by LCMV infection. Mice were injected intravenously with 100 PFU LCMV-WE. Sera were collected 48 h after infection and analyzed using an IFN-α4 ELISA kit (Performance Biomedical Laboratories).

Flow cytometry. Antibodies for flow cytometry were as follows: anti-CD4 (L3T4), anti-CD8 (53–6.7), anti-CD45R/B220 (RA3-6B2), anti-CD11c (HL3), anti-CD19 (1D3), anti–I-A^b (AF6-120.1), anti-CD11b (M1/70), anti-CD45 (30-F11), anti-CD25 (PC61), anti-CD69 (H1.2F3), anti-CD86 (GL1), anti-CD40 (3/23), anti–IFN-γ (XMG1.2), and anti–IL-17 (TC11-18H10; BD). Intracellular cytokine staining was done with the Cytofix/Cytoperm kit (BD). T cell proliferation was assessed by flow cytometry using an anti–human Ki67 staining kit (BD) containing anti-Ki67 (B56) and the isotype control (MOPC-21). Anti-Foxp3 (FJK-16s) and anti–PDCA-1 (BST-2, CD317) were obtained from eBioscience. Foxp3 staining was performed with the eBioscience kit.

T cell restimulation assays. 10^5 mononuclear LN and SC cells were incubated with 10^5 T cell–depleted splenocytes (Pan T isolation kit; Miltenyi Biotec) for 24 h in complete medium (RPMI and 10% FCS, supplemented with penicillin, streptomycin, L-glutamine, sodium pyruvate, and 2-mercaptoethanol) containing 100 μg/ml $MOG_{35–55}$. GolgiPlug (BD) was added for the final 4 h. Cells were analyzed by flow cytometry. IL-17, IFN-γ, IL-4, and IL-10 were measured in the culture supernatant using a Milliplex Mouse, cytokine 3plex (Millipore), or a Th1/Th2/Th17 Cytometric Bead Array (BD).

Ag presentation assays. Variable numbers of LN cDCs and pDCs were cultured with 10^5 CD4$^+$ 2D2 T cells in RPMI and 10% FCS in 96-well round-bottom plates. T cell activation was quantified after 18 h by flow cytometry using anti-CD69 antibodies.

In vitro T reg cell induction. 5×10^4 BM pDCs (CD11c^{int}B220$^+$PDCA-1$^+$) or BM cDCs (CD11c^{hi}B220$^-$PDCA-1$^-$) were incubated with 10 μM $MOG_{35–55}$ and stimulated with 3 μM CpG-A plus 3 μM CpG-B (InvivoGen) or 10 ng/ml LPS (Enzo Life Sciences, Inc.), respectively. 10^5 CD4$^+$ T cells from 2D2 × Foxp3-GFP mice were then added to the culture for 96 h.

Cell isolation. CD4$^+$ T cells were purified from LNs using a CD4$^+$ T cell purification kit (Miltenyi Biotec). Purified T cells were labeled with CMTMR or 10 μM CFSE (Invitrogen) before injection into the tail vein of recipient mice. cDCs and pDCs were purified from LNs by cell sorting using a FACSAria (BD). Mononuclear cells were isolated from the SC as previously described (Katz-Levy et al., 1999). BM pDCs and BM cDCs were generated as follows. After red cell lysis, BM cells were cultured for 7 d in complete RPMI medium containing 100 ng/ml of human Flt3L (PeproTech) for pDC generation or 20 ng/ml granulocyte-macrophage colony-stimulating factor (PeproTech) for cDC generation. pDCs and cDCs were further purified by sorting of CD11c^{int}B220$^+$PDCA-1$^+$ cells and CD11c^{hi}B220$^-$PDCA-1$^-$ cells, respectively, using a FACSVantage SE (BD).

Cytokine production by pDCs. BM-pDCs or pDCs purified from LNs were incubated for 24 h with CpG type A: ODN 1585 (5′-GGGGTCAACGTTGAGGGGGG-3′; InvivoGen). IFN-α4 was measured in the culture supernatants using an IFN-α4 ELISA kit (Performance Biomedical Laboratories). IL-6 and TNF were measured using a Mouse Inflammation Cytometric Bead Array (BD).

Immunofluorescence microscopy. Frozen LNs embedded in OCT (Sakura Finetek) were cut into 10-µm-thick sections. Sections were stained by standard procedures. Staining with anti-PNAd (MECA-79; BD) was revealed with Alexa Fluor 488–conjugated anti-IgM (Invitrogen). Alexa Fluor 647–conjugated anti–PDCA-1 was obtained from eBioscience. Pacific Blue–conjugated anti-Foxp3 (MF-14) was obtained from BioLegend. Sections were mounted with Mowiol fluorescent mounting medium (EMD). Images were acquired with a confocal microscope (LSM 510; Carl Zeiss, Inc.). pDC densities in LNs were determined using MetaMorph software (MDS Analytical Technologies).

Histological analysis of SCs. SCs were fixed by perfusion with paraformaldehyde (4%) and embedded in paraffin. Paraffin sections were stained with hematoxylin & eosin and Luxol fast blue. Frozen SCs were perfused with saline buffer and embedded in OCT (Sakura). Sections were stained by standard procedures using biotinylated anti-CD3ε (145-2C11; BD) and revealed with Alexa Fluor 488–conjugated streptavidin (Invitrogen).

Quantitative RT-PCR. LN $CD4^+$ T cells and pDCs were isolated 2 and/or 14 d after EAE induction. Total RNA was prepared with TRIzol (Invitrogen). cDNA was synthesized with random hexamers and Superscript II reverse transcription (Invitrogen). PCR was performed with the iCycler iQ Real-Time PCR Detection System and iQ SYBR green Supermix (Bio-Rad Laboratories). Results were quantified with a standard curve generated with serial dilutions of a reference cDNA preparation. GAPDH mRNA was used for normalization of IL-10 and TGF-β1 mRNA expression. β-actin mRNA was used for normalization of IFN-α4 mRNA expression. Primer sequences were as follows: IFN-α4 forward, 5′-CCTGTGTGATGCAGGAACC-3′ and reverse, 5′-TCACCTCCCAGGCACAGA-3′; IL-10 forward, 5′-GAATTCCCTGGGTGAGAAGC-3′ and reverse, 5′-CTCTTCACCTGCTCCACTGC-3′; TGF-β1 forward, 5′-AGGTCACCCGCGTGCTAATG-3′ and reverse, 5′-TCTGCACGGGACAGCAATGG-3′; β-actin forward, 5′-CAGAAGGAGATTACTGCTCTGGCT-3′ and reverse, 5′-GGAGCCACCGATCCACACA-3′; and GAPDH forward, 5′-CCCGTAGACAAAATGGTGAAG-3′ and reverse, 5′-AGGTCAATGAAGGGGTCGTTG-3′.

Statistics. Statistical significance was assessed by the two-tailed Student's *t* test, except for incidence of clinical EAE, for which statistical significance was assessed by the χ^2 test.

Online supplemental material. Fig. S1 shows the differential regulation of the gene encoding the MHC CIITA in cDCs, pDCs, and B cells. Fig. S2 shows a normal cytokine production by pIII+$IV^{-/-}$ pDCs. Fig. S3 shows that EAE exacerbation of in pIII+$IV^{-/-}$:WT chimeras is a consequence of deficient MOG presentation rather than altered IFN-α production by pDCs. Fig. S4 compares EAE histopathology in mice lacking or not MHCII expression by pDCs. Fig. S5 illustrates accentuated CNS inflammation during EAE in mice lacking MHCII expression by pDCs. Fig. S6 shows that the up-regulation of MHCII expression by activated microglia occurs normally during EAE in pIII+$IV^{-/-}$:WT chimeras. Fig. S7 shows a reduced T reg cell proliferation in the spleen of pIII+$IV^{-/-}$:WT chimeras during EAE. Table S1 shows that MHCII expression by pDCs induces the expansion of protective T reg cells. Online supplemental material is available at http://www.jem.org/cgi/content/full/jem.20092627/DC1.

We thank B. Becher for providing the recombinant mouse MOG, A.M. Lennon-Dumenil for critical reading of the manuscript, B. Huard, A. Kamath, and E. Belnoue for valuable discussions, and G. Schneiter, P. Fontannaz, S. Startchik, D. Wohlwend, L. Piriou, and S. Bichat for technical help.

Work in the laboratory was supported by the Swiss National Science Foundation (grant 3100A0-105895 to W. Reith; grant 310030-127042 to S. Hugues), the Geneva Cancer League, the Swiss Multiple Sclerosis Society, the National Center of Competence in Research on Neural Plasticity and Repair (NCCR-NEURO), and the EU FP6 consortium DC-THERA. M. Irla was supported by postdoctoral fellowships from the European Molecular Biology Organization and from the Roche and Novartis Research Foundations. S. Hugues was supported by the Institut National de la Santé et de la Recherche Médicale and by the Faculty of Medicine at the University of Geneva. Work in the laboratories of A. Fontana and T. Suter was supported by the Swiss National Science Foundation, the Swiss Multiple Sclerosis Society, and NCCR-NEURO. A. Fontana is Hertie Senior Research Professor Neuroscience of the Gemeinnützige Hertie-Stiftung. Work in the laboratory of P.H. Lalive was supported by the Swiss National Science Foundation and the Swiss Multiple Sclerosis Society.

The authors declare that they have no competing financial interests.

Submitted: 9 December 2009
Accepted: 8 July 2010

REFERENCES

Aloisi, F. 2001. Immune function of microglia. *Glia.* 36:165–179. doi:10.1002/glia.1106

Bailey, S.L., B. Schreiner, E.J. McMahon, and S.D. Miller. 2007. CNS myeloid DCs presenting endogenous myelin peptides 'preferentially' polarize CD4+ T(H)-17 cells in relapsing EAE. *Nat. Immunol.* 8:172–180. doi:10.1038/ni1430

Bailey-Bucktrout, S.L., S.C. Caulkins, G. Goings, J.A. Fischer, A. Dzionek, and S.D. Miller. 2008. Cutting edge: central nervous system plasmacytoid dendritic cells regulate the severity of relapsing experimental autoimmune encephalomyelitis. *J. Immunol.* 180:6457–6461.

Bajénoff, M., S. Granjeaud, and S. Guerder. 2003. The strategy of T cell antigen-presenting cell encounter in antigen-draining lymph nodes revealed by imaging of initial T cell activation. *J. Exp. Med.* 198:715–724. doi:10.1084/jem.20030167

Barnden, M.J., J. Allison, W.R. Heath, and F.R. Carbone. 1998. Defective TCR expression in transgenic mice constructed using cDNA-based alpha- and beta-chain genes under the control of heterologous regulatory elements. *Immunol. Cell Biol.* 76:34–40. doi:10.1046/j.1440-1711.1998.00709.x

Bettelli, E., M. Pagany, H.L. Weiner, C. Linington, R.A. Sobel, and V.K. Kuchroo. 2003. Myelin oligodendrocyte glycoprotein–specific T cell receptor transgenic mice develop spontaneous autoimmune optic neuritis. *J. Exp. Med.* 197:1073–1081. doi:10.1084/jem.20021603

Colonna, M., G. Trinchieri, and Y.J. Liu. 2004. Plasmacytoid dendritic cells in immunity. *Nat. Immunol.* 5:1219–1226. doi:10.1038/ni1141

Darrasse-Jèze, G., S. Deroubaix, H. Mouquet, G.D. Victora, T. Eisenreich, K.H. Yao, R.F. Masilamani, M.L. Dustin, A. Rudensky, K. Liu, and M.C. Nussenzweig. 2009. Feedback control of regulatory T cell homeostasis by dendritic cells in vivo. *J. Exp. Med.* 206:1853–1862. doi:10.1084/jem.20090746

de Heer, H.J., H. Hammad, T. Soullié, D. Hijdra, N. Vos, M.A. Willart, H.C. Hoogsteden, and B.N. Lambrecht. 2004. Essential role of lung plasmacytoid dendritic cells in preventing asthmatic reactions to harmless inhaled antigen. *J. Exp. Med.* 200:89–98. doi:10.1084/jem.20040035

Di Pucchio, T., B. Chatterjee, A. Smed-Sörensen, S. Clayton, A. Palazzo, M. Montes, Y. Xue, I. Mellman, J. Banchereau, and J.E. Connolly. 2008. Direct proteasome-independent cross-presentation of viral antigen by plasmacytoid dendritic cells on major histocompatibility complex class I. *Nat. Immunol.* 9:551–557. doi:10.1038/ni.1602

Fillatreau, S., C.H. Sweenie, M.J. McGeachy, D. Gray, and S.M. Anderton. 2002. B cells regulate autoimmunity by provision of IL-10. *Nat. Immunol.* 3:944–950. doi:10.1038/ni833

Gerdes, J., H. Lemke, H. Baisch, H.H. Wacker, U. Schwab, and H. Stein. 1984. Cell cycle analysis of a cell proliferation-associated human nuclear antigen defined by the monoclonal antibody Ki-67. *J. Immunol.* 133:1710–1715.

Goubier, A., B. Dubois, H. Gheit, G. Joubert, F. Villard-Truc, C. Asselin-Paturel, G. Trinchieri, and D. Kaiserlian. 2008. Plasmacytoid dendritic cells mediate oral tolerance. *Immunity.* 29:464–475. doi:10.1016/j.immuni.2008.06.017

Greter, M., F.L. Heppner, M.P. Lemos, B.M. Odermatt, N. Goebels, T. Laufer, R.J. Noelle, and B. Becher. 2005. Dendritic cells permit immune invasion of the CNS in an animal model of multiple sclerosis. *Nat. Med.* 11:328–334. doi:10.1038/nm1197

Hadeiba, H., T. Sato, A. Habtezion, C. Oderup, J. Pan, and E.C. Butcher. 2008. CCR9 expression defines tolerogenic plasmacytoid dendritic cells able to suppress acute graft-versus-host disease. *Nat. Immunol.* 9:1253–1260.

Hjelmström, P., A.E. Juedes, J. Fjell, and N.H. Ruddle. 1998. B-cell-deficient mice develop experimental allergic encephalomyelitis with demyelination after myelin oligodendrocyte glycoprotein sensitization. *J. Immunol.* 161:4480–4483.

Hoeffel, G., A.C. Ripoche, D. Matheoud, M. Nascimbeni, N. Escriou, P. Lebon, F. Heshmati, J.G. Guillet, M. Gannagé, S. Caillat-Zucman, et al. 2007. Antigen crosspresentation by human plasmacytoid dendritic cells. *Immunity.* 27:481–492. doi:10.1016/j.immuni.2007.07.021

Hugues, S., A. Boissonnas, S. Amigorena, and L. Fetler. 2006. The dynamics of dendritic cell-T cell interactions in priming and tolerance. *Curr. Opin. Immunol.* 18:491–495. doi:10.1016/j.coi.2006.03.021

Irla, M., S. Hugues, J. Gill, T. Nitta, Y. Hikosaka, I.R. Williams, F.X. Hubert, H.S. Scott, Y. Takahama, G.A. Holländer, and W. Reith. 2008. Autoantigen-specific interactions with CD4+ thymocytes control mature medullary thymic epithelial cell cellularity. *Immunity.* 29:451–463. doi:10.1016/j.immuni.2008.08.007

Isaksson, M., B. Ardesjö, L. Rönnblom, O. Kämpe, H. Lassmann, M.L. Eloranta, and A. Lobell. 2009. Plasmacytoid DC promote priming of autoimmune Th17 cells and EAE. *Eur. J. Immunol.* 39:2925–2935. doi:10.1002/eji.200839179

Jongbloed, S.L., R.A. Benson, M.B. Nickdel, P. Garside, I.B. McInnes, and J.M. Brewer. 2009. Plasmacytoid dendritic cells regulate breach of self-tolerance in autoimmune arthritis. *J. Immunol.* 182:963–968.

Katz-Levy, Y., K.L. Neville, A.M. Girvin, C.L. Vanderlugt, J.G. Pope, L.J. Tan, and S.D. Miller. 1999. Endogenous presentation of self myelin epitopes by CNS-resident APCs in Theiler's virus-infected mice. *J. Clin. Invest.* 104:599–610. doi:10.1172/JCI7292

Kitamura, D., J. Roes, R. Kühn, and K. Rajewsky. 1991. A B cell-deficient mouse by targeted disruption of the membrane exon of the immunoglobulin mu chain gene. *Nature.* 350:423–426. doi:10.1038/350423a0

Klein, L., K. Khazaie, and H. von Boehmer. 2003. In vivo dynamics of antigen-specific regulatory T cells not predicted from behavior in vitro. *Proc. Natl. Acad. Sci. USA.* 100:8886–8891. doi:10.1073/pnas.1533365100

Köntgen, F., G. Süss, C. Stewart, M. Steinmetz, and H. Bluethmann. 1993. Targeted disruption of the MHC class II Aa gene in C57BL/6 mice. *Int. Immunol.* 5:957–964. doi:10.1093/intimm/5.8.957

Korn, T., J. Reddy, W. Gao, E. Bettelli, A. Awasthi, T.R. Petersen, B.T. Bäckström, R.A. Sobel, K.W. Wucherpfennig, T.B. Strom, et al. 2007. Myelin-specific regulatory T cells accumulate in the CNS but fail to control autoimmune inflammation. *Nat. Med.* 13:423–431. doi:10.1038/nm1564

Lampropoulou, V., K. Hoehlig, T. Roch, P. Neves, E. Calderón Gómez, C.H. Sweenie, Y. Hao, A.A. Freitas, U. Steinhoff, S.M. Anderton, and S. Fillatreau. 2008. TLR-activated B cells suppress T cell-mediated autoimmunity. *J. Immunol.* 180:4763–4773.

Lande, R., V. Gafa, B. Serafini, E. Giacomini, A. Visconti, M.E. Remoli, M. Severa, M. Parmentier, G. Ristori, M. Salvetti, et al. 2008. Plasmacytoid dendritic cells in multiple sclerosis: intracerebral recruitment and impaired maturation in response to interferon-beta. *J. Neuropathol. Exp. Neurol.* 67:388–401.

Langrish, C.L., Y. Chen, W.M. Blumenschein, J. Mattson, B. Basham, J.D. Sedgwick, T. McClanahan, R.A. Kastelein, and D.J. Cua. 2005. IL-23 drives a pathogenic T cell population that induces autoimmune inflammation. *J. Exp. Med.* 201:233–240. doi:10.1084/jem.20041257

Lebedeva, T., M.L. Dustin, and Y. Sykulev. 2005. ICAM-1 co-stimulates target cells to facilitate antigen presentation. *Curr. Opin. Immunol.* 17:251–258. doi:10.1016/j.coi.2005.04.008

LeibundGut-Landmann, S., J.M. Waldburger, C. Reis e Sousa, H. Acha-Orbea, W. Reith, and W. Reith. 2004. MHC class II expression is differentially regulated in plasmacytoid and conventional dendritic cells. *Nat. Immunol.* 5:899–908. doi:10.1038/ni1109

Matsushita, T., K. Yanaba, J.D. Bouaziz, M. Fujimoto, and T.F. Tedder. 2008. Regulatory B cells inhibit EAE initiation in mice while other B cells promote disease progression. *J. Clin. Invest.* 118:3420–3430.

Murphy, C.A., C.L. Langrish, Y. Chen, W. Blumenschein, T. McClanahan, R.A. Kastelein, J.D. Sedgwick, and D.J. Cua. 2003. Divergent pro- and antiinflammatory roles for IL-23 and IL-12 in joint autoimmune inflammation. *J. Exp. Med.* 198:1951–1957. doi:10.1084/jem.20030896

O'Connor, R.A., and S.M. Anderton. 2008. Foxp3+ regulatory T cells in the control of experimental CNS autoimmune disease. *J. Neuroimmunol.* 193:1–11. doi:10.1016/j.jneuroim.2007.11.016

Ochando, J.C., C. Homma, Y. Yang, A. Hidalgo, A. Garin, F. Tacke, V. Angeli, Y. Li, P. Boros, Y. Ding, et al. 2006. Alloantigen-presenting plasmacytoid dendritic cells mediate tolerance to vascularized grafts. *Nat. Immunol.* 7:652–662. doi:10.1038/ni1333

Pashenkov, M., Y.M. Huang, V. Kostulas, M. Haglund, M. Söderström, and H. Link. 2001. Two subsets of dendritic cells are present in human cerebrospinal fluid. *Brain.* 124:480–492. doi:10.1093/brain/124.3.480

Reith, W., S. LeibundGut-Landmann, and J.M. Waldburger. 2005. Regulation of MHC class II gene expression by the class II transactivator. *Nat. Rev. Immunol.* 5:793–806. doi:10.1038/nri1708

Sapoznikov, A., J.A. Fischer, T. Zaft, R. Krauthgamer, A. Dzionek, and S. Jung. 2007. Organ-dependent in vivo priming of naive CD4+, but not CD8+, T cells by plasmacytoid dendritic cells. *J. Exp. Med.* 204:1923–1933. doi:10.1084/jem.20062373

Skupsky, J., A.H. Zhang, Y. Su, and D.W. Scott. 2010. B-cell-delivered gene therapy induces functional T regulatory cells and leads to a loss of antigen-specific effector cells. *Mol. Ther.* In press.

Stasiolek, M., A. Bayas, N. Kruse, A. Wieczarkowiecz, K.V. Toyka, R. Gold, and K. Selmaj. 2006. Impaired maturation and altered regulatory function of plasmacytoid dendritic cells in multiple sclerosis. *Brain.* 129:1293–1305. doi:10.1093/brain/awl043

Steinman, L., R. Martin, C. Bernard, P. Conlon, and J.R. Oksenberg. 2002. Multiple sclerosis: deeper understanding of its pathogenesis reveals new targets for therapy. *Annu. Rev. Neurosci.* 25:491–505. doi:10.1146/annurev.neuro.25.112701.142913

Steinman, R.M., D. Hawiger, and M.C. Nussenzweig. 2003. Tolerogenic dendritic cells. *Annu. Rev. Immunol.* 21:685–711. doi:10.1146/annurev.immunol.21.120601.141040

Suter, T., U. Malipiero, L. Otten, B. Ludewig, A. Muelethaler-Mottet, B. Mach, W. Reith, and A. Fontana. 2000. Dendritic cells and differential usage of the MHC class II transactivator promoters in the central nervous system in experimental autoimmune encephalitis. *Eur. J. Immunol.* 30:794–802. doi:10.1002/1521-4141(200003)30:3<794::AID-IMMU794>3.0.CO;2-Q

Urich, E., I. Gutcher, M. Prinz, and B. Becher. 2006. Autoantibody-mediated demyelination depends on complement activation but not activatory Fc-receptors. *Proc. Natl. Acad. Sci. USA.* 103:18697–18702. doi:10.1073/pnas.0607283103

Villadangos, J.A., and L. Young. 2008. Antigen-presentation properties of plasmacytoid dendritic cells. *Immunity.* 29:352–361. doi:10.1016/j.immuni.2008.09.002

Waldburger, J.M., S. Rossi, G.A. Hollander, H.R. Rodewald, W. Reith, and H. Acha-Orbea. 2003. Promoter IV of the class II transactivator gene is essential for positive selection of CD4+ T cells. *Blood.* 101:3550–3559. doi:10.1182/blood-2002-06-1855

Wekerle, H. 2008. Lessons from multiple sclerosis: models, concepts, observations. *Ann. Rheum. Dis.* 67:iii56–iii60. doi:10.1136/ard.2008.098020

Wekerle, H., D. Sun, R.L. Oropeza-Wekerle, and R. Meyermann. 1987. Immune reactivity in the nervous system: modulation of T-lymphocyte activation by glial cells. *J. Exp. Biol.* 132:43–57.

Young, L.J., N.S. Wilson, P. Schnorrer, A. Proietto, T. ten Broeke, Y. Matsuki, A.M. Mount, G.T. Belz, M. O'Keeffe, M. Ohmura-Hoshino, et al. 2008. Differential MHC class II synthesis and ubiquitination confers distinct antigen-presenting properties on conventional and plasmacytoid dendritic cells. *Nat. Immunol.* 9:1244–1252. doi:10.1038/ni.1665